Enhancing disaster risk resilience using greenspace in urbanising Quito, Ecuador

C. Scott Watson[1], John R. Elliott[1], Susanna K. Ebmeier[1], María Antonieta Vásquez[2], Camilo Zapata[2], Santiago Bonilla-Bedoya[3], Paulina Cubillo[4], Diego Francisco Orbe[4], Marco Córdova[5], Jonathan Menoscal[5], Elisa Sevilla[2]

[1]COMET, School of Earth and Environment, University of Leeds, Leeds, LS2 9JT, UK.

[2]College of Social Sciences and Humanities, Universidad San Francisco de Quito, Quito 170901, Ecuador.

[3]Research Center for the Territory and Sustainable Habitat, Universidad Tecnológica Indoamérica, Machala y Sabanilla, 170301, Quito, Ecuador.

[4]Centro de Información Urbana de Quito - CIUQ, Quito, Ecuador.

[5]Facultad Latinoamericana de Ciencias Sociales - Flacso, Quito, Ecuador.

Correspondence to: C. Scott Watson (c.s.watson@leeds.ac.uk)

Abstract

Greenspaces within broader ecosystem-based disaster risk reduction strategies (Eco-DRR) provide multiple benefits to society, biodiversity, and addressing climate breakdown. In this study, we investigated urban growth, its intersection with hazards, and the availability of greenspace for disaster risk reduction (DRR) in the city of Quito, Ecuador, which experiences multiple hazards including landslides, floods, volcanoes, and earthquakes. We used satellite data to quantify urban sprawl and developed a workflow incorporating high resolution digital elevation models (DEMs) to identify potential greenspaces for emergency refuge accommodation (DRR greenspace), for example following an earthquake. Quito's historical urban growth totalled ~192 km^2 1986–2020 and was primarily on flatter land crossed by deep ravines. By contrast, future projections indicate an increasing intersection between easterly urbanisation and steep areas of high landslide susceptibility. Therefore, a timely opportunity exists for future risk-informed planning. Our workflow identified 18.6 km^2 of DRR greenspaces, of which 16.3 km^2 intersected with potential sources of landslide and flood hazards, indicating that hazard events could impact potential 'safe spaces'. These spaces could mitigate future risk if designated as greenspaces and left undeveloped. DRR greenspace overlapped 7% (2.5 km^2) with municipality designated greenspace. Similarly, 10% (1.7 km^2) of municipality designated 'safe space' for use following an earthquake was classified as potentially DRR suitable in our analysis. For emergency refuge, currently designated greenspaces could accommodate ~2–14% of Quito's population within 800 m. This increases to 8–40% considering all the potential DRR greenspace mapped in this study. Therefore, a gap exists

31 between the provision of DRR and designated greenspace. Within Quito, we found a disparity between access to greenspaces

32 across socio-economic groups with lower income groups having less access and further to travel to designated greenspaces.

33 Notably, the accessibility of greenspaces was high overall with 98% (2.3 million) of Quito's population within 800 m of a

34 designated greenspace, of which 88% (2.1 million) had access to potential DRR greenspaces. Our workflow demonstrates a

35 citywide evaluation of DRR greenspace potential and provides the foundation upon which to evaluate these spaces with local

36 stakeholders. Promoting equitable access to greenspaces, communicating their multiple benefits, and considering their use to

37 restrict propagating development into hazardous areas are key themes that emerge for further investigation.

1 Introduction

39 Urbanising and increasing populations are a global trend that create a range of societal and environmental challenges

40 including food and water security (Godfray et al., 2010; Hoekstra et al., 2018), air pollution (Fenger, 1999; Escobedo and

41 Nowak, 2009; Zalakeviciute et al., 2018), disease (Marmot et al., 2008), loss of biodiversity (McDonald et al., 2020), climate

42 change (De Sherbinin et al., 2007; Flörke et al., 2018), and exposure to disaster risk (Pelling et al., 2004). Approximately

43 68% of the world's population are projected to live in urban areas by 2050, many of which are yet to be developed, and the

44 rate of urbanisation is greatest for developing countries (UN DESA, 2019). Development of informal settlements takes place

45 outside of regulatory frameworks such as land use planning or building design codes (UN-Habitat, 2003; Oliver-Smith et al.,

46 2016). Therefore, urbanisation often occurs within or creates hazardous areas, which exacerbates the socioeconomic

47 inequalities of disaster risk due to overcrowding, unsafe housing, and lack of infrastructure and services (Baker, 2012;

48 Cardona et al., 2012). Reducing disaster risk and losses is the aim of the global Sendai Framework for Disaster Risk

49 Reduction 2015–2030 (UNDRR, 2015) and is integral to the goal of building sustainable cities and communities (UN

50 General Assembly, 2015). Additionally, nature-based solutions (NbS) involving greenspace in cities are increasingly

51 recognised within a framework of Ecosystem-based Disaster Risk Reduction (Eco-DRR) (Estrella and Saalismaa, 2013;

52 Faivre et al., 2018; UNDRR, 2020) and can be designed and monitored using an increasing number of earth observation

53 (EO) technologies (Kumar et al., 2021). EO data are widely used for land cover classifications to quantify historical trends in

54 urban expansion and to model future urbanisation projections (Schneider and Woodcock, 2008; Bonilla-Bedoya et al.,

55 2020b). Both high-resolution (< 1 m, commercial) (Myint et al., 2011; Georganos et al., 2018) and medium resolution (10–

56 30 m, open-access) (e.g. Landsat and Sentinel-2) optical satellite imagery are used for land cover and greenspace mapping

57 (Fuller et al., 1994; Labib and Harris, 2018; Deng et al., 2019).

58

59 There are multiple definitions of greenspace, however, they generally include reference to public parks, gardens, open space,

60 wetlands, street verges, woodland, and sports grounds (Taylor and Hochuli, 2017). Greenspace is associated with multiple

61 impacts on urban and natural systems (Fig. 1) including: improving mental and physical health (James et al., 2015; WHO

62 Regional Office for Europe, 2016; Marselle et al., 2020; Bauwelinck et al., 2021); conserving natural ecosystems and

63   biodiversity (Aronson et al., 2017; McDonald et al., 2020); creating economic opportunities (Gregory McPherson, 1992);
64   building community resilience to hazards (Colding and Barthel, 2013), including reducing landslide risk (Phillips and
65   Marden, 2005; Sandholz et al., 2018) and urban flooding (Maragno et al., 2018); and providing safe spaces in the event of a
66   disaster (Shrestha et al., 2018; Sphere Association, 2018; Shimpo et al., 2019; Jeong et al., 2021). However, greenspace
67   planning in urban environments is often recreation focused (Boulton et al., 2018). Therefore, it is important to recognise the
68   provision of multi-benefit greenspaces within an Eco-DRR framework, and the diverse accessibility, ownership, and
69   management of such spaces (Colding and Barthel, 2013). Similarly, the creation and designation of greenspace requires
70   consideration of social justice issues, such as the impact on property values (Wolch et al., 2014; García-Lamarca et al.,
71   2020).

72

73   Green cities, which incorporate diverse greenspace, green infrastructure, and interconnected social and ecological networks,
74   provide opportunities to enhance disaster resilience and deliver multiple benefits for sustainable development and nature
75   conservation (Benedict and MacMahon, 2002; Tidball and Krasny, 2012). These elements may be designed and integrated
76   into planning policy (Jeong et al., 2021) or emerge following crises, such as loss of food security prompting the proliferation
77   of urban gardening (Altieri et al., 1999; Gonzalez, 2003; Colding and Barthel, 2013). Similarly, following disaster events
78   such as earthquakes, open spaces are used for emergency refuge (Allan et al., 2013; Borland, 2020). The latter point was the
79   case following the 2015 Gorkha earthquake where greenspaces were used for temporary accommodation away from
80   collapsed and damaged buildings (Fig. 1 b-c). Temporary government camps homed over 30,000 people in the Kathmandu
81   Valley and over 1,000 smaller shelter sites homed thousands more (Khazai et al., 2015). Greenspace was also prioritised in
82   Tokyo following the 1923 Great Kantō Earthquake, where parks originally designed to provide space for children were later
83   valued as emergency refuges (Borland, 2020). Innovative greenspace design elements may also emerge following disaster
84   events, such as integrating water bodies and pumps, edible plant species, and multi-purpose (e.g. seating, dining, and
85   cooking) communal seating areas into greenspace areas (Bryant and Allan, 2013).

86

87   Historically, green space in Quito was defined by the rural-urban relationship. Until the end of the 19th century, green spaces
88   were the "Ejidos", sites for agriculture and livestock, which were located on the outskirts of the city. The urbanisation model
89   did not contemplate green spaces in its design and natural spaces such as the ravines were mostly filled in (Aragundi et al.,
90   2016). This is important because parks and plazas have been repeatedly used as refuge sites after earthquakes in Quito. For
91   example, during the 1859 Quito earthquake and 1868 Ibarra earthquake, refugee tents were set in the main plazas and parks
92   of the city (e.g. Figure 1d, e). During the 20th Century, the use of these greenspaces and open spaces like plazas as refuge
93   after earthquakes was recognised through the creation of official 'safe spaces' (see section 4.3) (Metro Ecuador, 2019).

94
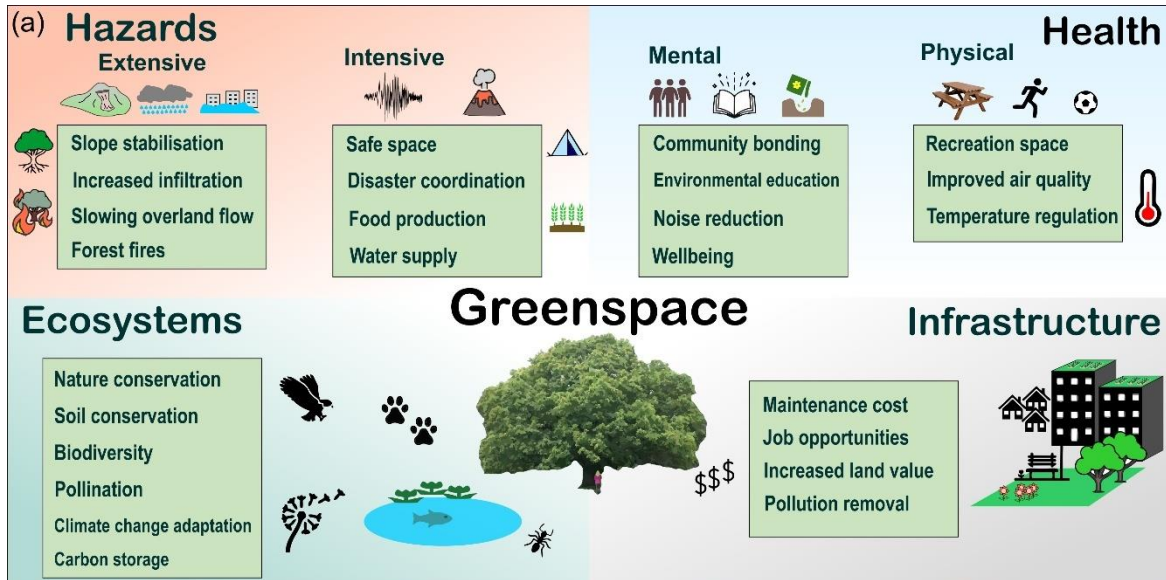
Figure 1: (a) Example impacts of urban greenspace on hazards, health, ecosystems, and infrastructure. (b-c) An area of greenspace 'Tundikhel' (Lat: 27.702°, Lon: 85.315°) in Kathmandu, Nepal, which was used for temporary tented accommodation following the Gorkha earthquake (25 April 2015). (d-e) Tents in Plaza Santo Domingo and Plaza Mayor (Plaza Grande) in Quito after the 1868 Ibarra earthquake.

Quito has a population of over 2 million (2020), having doubled in just three decades from 1 million in the late 1980s, and which is projected to exceed 3.4 million by 2040 (DMQ, 2018). The expansion of formal and informal settlements into hazardous areas increases disaster risk from events including landslides, flooding, volcanic eruptions, and earthquakes. Increased disaster risk is due to both increased exposure to natural hazards and the social vulnerability of the exposed communities (e.g. Valcárcel et al., 2017). Therefore, in this study we assessed the potential of greenspace for reducing disaster risk in contemporary Quito, and for guiding the development of more resilient communities in future urban areas. Specifically, we: (1) quantified Quito's recent historical urban expansion using satellite-based optical imagery and evaluated potential future urbanisation scenarios using land classification metrics; (2) investigated the intersection between the built environment and natural hazards; and (3) evaluated the potential role of urban greenspace for reducing disaster risk in Quito by providing 'safe spaces'. In this study, we define a style of greenspace relevant to disaster risk reduction that is quantifiable using optical satellite data.

2 Study region

Quito, Ecuador is situated just south of the equator in the Inter-Andean Valley of South America at over 2,800 m a.s.l. and is bounded by Pichincha Volcano (4794 m) to the west and steep topography to the east (Fig. 2). Topography and factors such as the intertropical convergence zone and the South Atlantic convergence zone determine Quito's climate (Hastenrath, 1997; Vincenti et al., 2012; Zambrano-Barragán et al., 2011). Quito's precipitation distribution has two modalities, March–April and October–December, with an average annual precipitation of 1200 mm and an average annual temperature of 13.4°C (Vincenti et al., 2012; Zambrano-Barragán et al., 2011). In recent decades, Quito's urban extent has spread many kilometres to the north, east, and south (Bonilla-Bedoya et al., 2020b; Salazar et al., 2020). Westward expansion is limited, although not absent, due to the designated protected areas on the slopes of Pichincha volcano, which were implemented following urban encroachment and the incidence of landslides and floods (Vidal et al., 2015; DMQ, 2018). Urban expansion is changing Quito's exposure to natural hazards including landslides, floods, volcanic activity, and earthquakes (Chatelain et al., 1999; Hall et al., 2008; Carmin and Anguelovski, 2009; Valcárcel et al., 2017). Quito's urban area now exceeds the current Metropolitan District of Quito (DMQ) administrative boundary (Bonilla-Bedoya et al., 2020a; Salazar et al., 2021). Therefore, in this study, we define two separate areas of interest (AOIs): (1) a 'land cover AOI' for mapping land cover change, which encompasses the core urban area of Quito, and (2) a 'city AOI' for mapping greenspace, which includes the Administrative Level 3 Parishes of Quito, Cumbaya, Llano Chico, Calderon (Carapungo), Conocoto, Zambiza, and Nayon (Fig. 2a, S1).

128
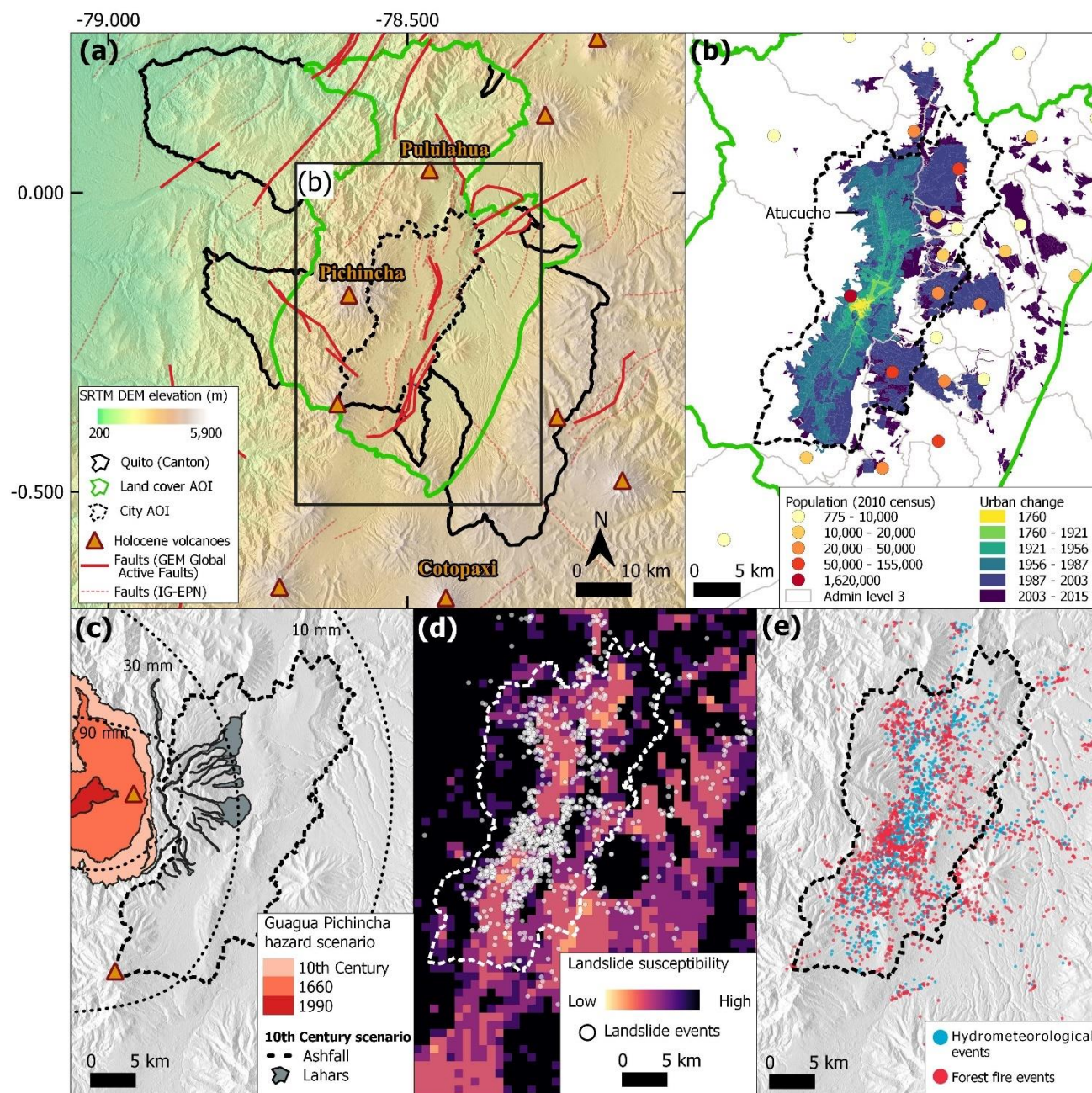
Figure 2: (a) The location of Quito, Ecuador in relation to regional seismic faults and volcanoes. Fault lines (red) are from the Geophysical Institute of the National Polytechnic School (IG-EPN) and Global Earthquake Model Global Active Faults (Styron, 2019). (b) Urban change and population of Quito are mapped using Open Government data (http://gobiernoabierto.quito.gob.ec/). (c) Volcanic hazards from the IG-EPN et al. (2019) Pichincha Volcano hazard map. (d) Landslide susceptibility map (Stanley and Kirschbaum, 2017) and observed landslide events (n=1,321) (2006–2017) (http://gobiernoabierto.quito.gob.ec/). (e) Observed Hydrometeorological (n=1,574) and forest fire events (n=2,358) (2006–2017) (http://gobiernoabierto.quito.gob.ec/).

135

136 Landslides and floods are both extensive natural hazards in Quito owing to the steep topography, intense rainfall, and filling
137 of natural drainage channels to create building space (DMQ, 2018; Castelo et al., 2018; Domínguez-Castro et al., 2018).
138 Landslides are concentrated on the steep slopes of Quito's periphery and ravines (Fig. 2d), whereas flood events are spread
139 across Quito's urban extent (Fig. 2e). Although less frequent, volcanic eruptions and earthquakes pose significant risk to
140 large populations. Quito lies 12 km from the active volcano Guagua Pichincha, where activity over the past decades has been
141 characterised by small explosions, ash and gas emission (Loughlin et al., 2015). Past eruptions have covered Quito in ash, for
142 example, the 1660 eruption ash deposits are ~10 cm thick in central Quito (Robin et al., 2008). Recent pyroclastic flows and
143 surges have been channelled by topography away from Quito to the west, but potential volcanic hazards in Quito include
144 secondary lahars as well as ashfall, which are mapped using knowledge of historic eruptions (IG-EPN, 2019) (Fig. 2c).
145 Quito's road network, and water supply, are also all vulnerable to flows and especially ash from multiple volcanoes (Wilson
146 et al., 2012; Loughlin et al., 2015). The Global Earthquake Model estimates (Pagani et al., 2018) at the regional scale
147 indicate a relatively high seismic hazard with a Peak Ground Acceleration (PGA) of 0.55-0.9 g (with a 10% probability of
148 exceedance in 50 years) (Fig. S1). Similarly, Beauval (2018) estimate a PGA of ~0.4-0.6 g or Quito in a return period of 475
149 years. The Quito Fault System creates seismic hazard across the city, with a maximum earthquake size estimated at M_w 6.6
150 and a recurrence time of ~150-435 years (Alvarado et al., 2014). Earthquake scenario damage models show that the highest
151 rates of potential building damage are associated with areas of highest social vulnerability (Valcárcel et al., 2017). Multi-
152 hazards or cascading hazards could emerge through combinations of single hazards, such as a volcanic eruption that deposits
153 ash on slopes and blocks urban drains, which if followed by heavy rain could produce lahars and urban flooding respectively
154 (Gill et al., 2021).

156 In terms of policy and planning, the issue of green space in the city currently maintains a spatial-functional emphasis,
157 although environmental (mainly related to climate change) and socio-political (public space, right to the city) criteria have
158 been incorporated. There was an important change in the first urban plan of the city (1942), where the design envisages a
159 series of green spaces, especially in the north of the city, under a criterion of recreational and sports spaces. This is the case
160 of the current La Carolina park, which was initially the city's racecourse. The plan also considered a series of smaller green
161 spaces within the residential areas. However, a balanced development between urbanisation and the environment was not
162 planned, but rather green and open spaces in general were thought of as part of the zoning logic of the time. This model of
163 urban development between the 1970s and 2000s is the main risk factor for disasters in the city (Carrión and Erazo Espinosa,
164 2012). In 1993, the Metropolitan District of Quito (DMQ) was created, with 9.3% of its territory being urban and 90.7%
165 rural. This new territorial configuration is relevant because both planning and risk analysis tend to concentrate only on the
166 urbanised area (Peralta Arias and Higueras García, 2016).

168 When outlining the vision of Quito to year 2040, the Municipality of the Metropolitan District of Quito recognised the
169 importance of an urban green network for delivering social and natural benefits, including risk mitigation (DMQ, 2018). This

recognition of greenspace to reduce risk from morphoclimatic events has been present in the planning instruments of the Municipality since the 1980s. The destructive mudflows of 1983 on the slopes of Pichincha that had been previously urbanised by informal settlements prompted the national government of Ecuador to legislate for the law on "protective forests". These forests were designed to prevent erosion, mitigate landslides, and control informal urbanisation on slopes around Quito. According to Sierra (2009), the role of greenspace in the borders of the city were first designed as recreational and patrimonial landscapes from 1940s onwards, and later, in the 1970s and 1980s incorporated environmental, city growth control, and risk mitigation properties. In the last 30 years, there has been Municipal and community interest in the recovery of ravines for recreational activities and improving citizens quality of life by implementing nature-based solutions alongside urban development; however, its realisation and impact has been small at the city scale, instead confined to planning-stage pilot projects such as in the San Enrique de Velasco district in the northwest of Quito (Salmon et al., 2021).

3 Methodology

3.1 Urban growth

Urban growth for the period 1986 to 2020 was derived by applying a land cover classification workflow to 30 m resolution Landsat satellite imagery (Fig. 3), including Landsat 4 Thematic Mapper (TM), Landsat 7 Enhanced Thematic Mapper Plus (ETM+), and Landsat 8 Operational Land Imager (OLI). Landsat imagery was selected June to September to avoid cloud cover during the wet season (Domínguez-Castro et al., 2018). Therefore, seasonal spectral variations in land covers are not captured. Images were pre-processed using Landsat-based detection of Trends in Disturbance and Recovery (LandTrendr) and Google Earth Engine to create multi-image mosaics with minimal cloud cover using a medoid pixel composite (Gorelick et al., 2017; Kennedy et al., 2018). Training data were manually digitised as 500 polygons (median polygon area of 5,400 m^2) with reference to the 1986 image using four classes: 1) urban, 2) woodland, 3) scrub vegetation and bare ground, and 4) agriculture and grassland. Training data were masked using the normalised difference vegetation index (NDVI) vegetation loss and growth masks that are output from LandTrendr to leave areas of training data that were spectrally consistent through time (1986–2020). Landsat composites were stacked with elevation and slope layers derived from the 30 m Shuttle Radar Topography Mission (SRTM) digital elevation model (DEM) (Farr et al., 2007) since these additional variables were shown to improve land cover classification performance (Zhu et al., 2016). We used a Random Forest classification, which is a decision tree approach popular for land cover classifications owing to their high accuracy, broad data handling, and low sensitivity to training data noise (Rodriguez-Galiano et al., 2012; Zhu et al., 2016). The Orfeo Toolbox Random Forest classifier (Inglada and Christophe, 2009) (Table S1) was run 50 times for each time period using 200 trees and a random sample of training data to account for imbalance between classes (Millard and Richardson, 2015) (Table S1). The modal value was used to produce the final classification map, which was accuracy assessed using an independent stratified random sample of 200 reference points in each class created using high resolution satellite imagery (Fig. S2). High resolution multispectral satellite imagery was not available in the 1980s, which reduces classification confidence in training and

reference data, however, a panchromatic ~1 m resolution aerial orthophoto of Quito in 1977 from Instituto Geográfico Militar (1977) was used for reference. The accuracy assessment was used to produce an error-adjusted area and confidence interval of each land cover classification (e.g. Olofsson et al., 2013; Olofsson et al., 2014).

Future urbanisation scenarios in Quito were assessed with reference to Bonilla-Bedoya et al. (2020b) and Salazar et al. (2020). Both studies used predictor variables to model future urbanisation scenarios in Quito. Salazar et al. (2020) present a scenario to the year 2050, whereas Bonilla-Bedoya et al. (2020b) define an 'urbanisation probability' without a scenario end date. Nonetheless, the spatial trends in both studies are similar. Predictors used to derive urbanisation probability included biophysical (e.g. precipitation, slope, and altitude), land cover and management (e.g. protected areas), infrastructure and services (e.g. road network), socioeconomic (e.g. land value), and landscape metrics (e.g. landscape patch size and shape) (Bonilla-Bedoya et al., 2020). We used 'high' (urbanisation probability: 55–79 %) and 'very high' (urbanisation probability: 79–100 %) classes from Bonilla-Bedoya et al. (2020b) in this study (Fig. S3) to evaluate future land cover scenarios and the intersection of urban areas with hazards.
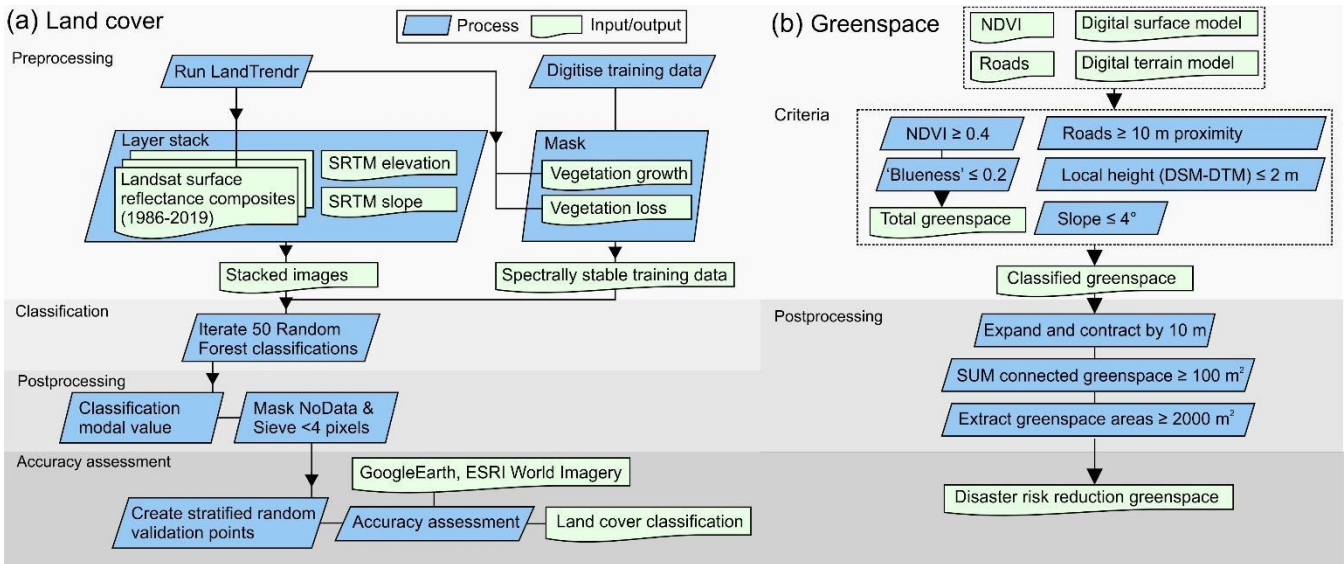
Figure 3: (a) Land cover classification and accuracy assessment workflow. (b) Classification of greenspace that could potentially contribute to disaster risk reduction (DRR), herein 'DRR greenspace'.

3.2 Topography

The 30 m SRTM DEM was used to extract statistics on the elevation and slope within the land cover change area of interest (AOI) (Fig. 2a). A higher resolution (2 m and 10 m) DEM and orthoimagery was created for a smaller AOI (Fig. 2a), which bounded the Administrative Level 3 Parishes of Quito, Cumbaya, Llano Chico, Calderon (Carapungo), Conocoto, Zambiza, and Nayon. This AOI was covered by tristereo Pleiades imagery, which were acquired on five separate dates (5th November

224 2019, 28th January 2020, 9th February 2020, 6th June 2020, and 28th July 2020) in both panchromatic (~0.7 m) and multi-

225 spectral (~2.8 m RGB and Near Infrared) modes (Table S2). Tristereo acquisitions produce elevation models with lower

226 uncertainties compared to bistereo acquisitions due to greater point cloud densities afforded by the extra viewing angle

227 (Zhou et al., 2015). All imagery was delivered with radiometric processing to reflectance and supplied with rational

228 polynomial coefficients (RPCs) (Airbus Defence and Space, 2012). Agisoft Metashape v.1.6.5 was used to process the

229 imagery to create a DEM, digital terrain model (DTM), and orthorectified imagery. Briefly: (1) the panchromatic and

230 multispectral imagery were aligned in one bundle to produce a sparse point cloud; (2) the sparse cloud was filtered to remove

231 outliers using Metashape's gradual selection tools; (3) a dense point cloud was constructed using the panchromatic imagery,

232 which was used to create a 2 m resolution DEM and (4) orthorectify the satellite imagery. Metashape's ground classification

233 (maximum angle: 15°, maximum distance: 0.5 m, cell size: 50 m) was applied to the dense cloud and used to create the

234 DTM. An additional DSM was output at 10 m resolution to reduce data gaps for deriving a Topographic Wetness Index

235 (TWI) (Section 3.3).

236

237 The accuracy of the Pleiades DEM was assessed using Ice, Cloud and land Elevation Satellite (ICESAT-2) altimetry data.

238 ICESAT-2 data has an expected vertical accuracy that is lower than the error expected from a Pleiades DEM created without

239 ground control points (> 3–5m) (Passalacqua et al., 2015; Markus et al., 2017) and was therefore used as an independent

240 validation check. We extracted High Confidence returns from the Advanced Topographic Laser Altimeter System (ATLAS)

241 instrument ATL03 Global Geolocated Photon Height data acquired 6th December 2018 to 3rd June 2020 that intersected with

242 the Pleiades data (Neumann et al., 2019; Neumann, 2020). Photons were filtered to exclude slopes steeper than 20° and

243 aggregated into 5 m grid cell mean values. Cells containing ≥ 2 photons with an elevation range ≤1 m, were carried forward

244 for the validation (n = 11,922). We coregistered the Pleiades DEM and gridded ICESAT-2 data following the x, y, z shift

245 correction of Nuth and Kääb (2011) and the difference in elevation values were compared. The mean vertical difference

246 between the ICESAT-2 and Pleiades data was 0.38 m (one standard deviation: 1.32 m) with a normalised median absolute

247 deviation of 0.84 m.

248 **3.3 Hazards**

249 Information on natural hazards affecting Quito were collated from published sources and Ecuador's Open Government data.

250 We used a global landslide susceptibility model that was validated against local and global landslide inventories, with an

251 emphasis on rainfall-triggered events (Kirschbaum et al., 2016; Stanley and Kirschbaum, 2017). Landslide susceptibility was

252 ranked on a scale of 1 (low) to 5 (high) and the model combined data on slope, faults, geology, forest loss, and road

253 networks, aggregated to ~1 km grid cells (Stanley and Kirschbaum, 2017). Open Government records of 'Accidents' 2006–

254 2017 were used to identify the geographic distribution of mass movement events (n = 1,321), which were compared to the

255 global landslide susceptibility model (Fig. S4) (Ministry of Territory. Habitat and Housing., 2020). We masked Class 5

256 (high) of the landslide susceptibility model out of the future urbanisation scenario of Bonilla-Bedoya et al. (2020b) to create

257 a restricted scenario of urban growth, which reflects DMQ's vision to remove high risk areas from future land occupation.

258 We also excluded development on the slopes of Pichincha volcano (as unrealistically inaccessible given steep slopes) and

259 included an area of development spanning the Metropolitan District boundary in the south (Fig. S3). We refer to the original

260 scenario of future urbanisation and the modified scenario as F-U and M-U respectively. Information on volcanic hazards

261 were obtained from the Geophysical Institute of the National Polytechnic School (IG-EPN) through the National Information

262 System (SNI) (SNI, 2020). Spatial variation in earthquake hazard across Quito was not explored in this study due to the

263 coarse resolution (~10 km) of available hazard information (Fig. S1). However, the high regional seismic hazard (Alvarado

264 et al., 2014; Pagani et al., 2018) motivates our city-wide analysis of greenspace.

265

266 The 10 m Pleiades DEM was hydrologically corrected by breaching sinks (Lidberg et al., 2017), using the *Breach*

267 *depressions least cost tool* of Whitebox 1.4.0. The breached DEM was used to derive a TWI, which was intersected with

268 flood events in the Open Government database (n = 1,274) to assess whether high TWI values correspond to greater

269 incidences of flood events, and therefore was indicative of potential flood hazard (Jalayer et al., 2014; Kelleher and

270 McPhillips, 2020).

271

272 $$TWI = \ln\left(\frac{a}{tan\beta}\right) \qquad (1)$$

273

274

275 where *a* represents the specific catchment area and *tanβ* represents the local DEM slope. Therefore, the TWI describes the

276 tendency for a cell to accumulate and evacuate water (Beven and Kirkby, 1979; Manfreda et al., 2011; Mattivi et al., 2019).

277 We assumed a positional uncertainty radius of 20 m in the flood event records based on the observed positional spread of

278 recorded traffic collisions at road junctions in the same database (Fig. S5). The maximum TWI value within a 20 m radius of

279 the recorded point was extracted and compared to the TWI for a random sample of 10,000 points to test whether there was a

280 statistically significant difference in the TWI at locations of flood events (e.g. Kelleher and McPhillips, 2020).

281 **3.4 Greenspace**

282 Orthorectified multi-spectral Pleiades imagery was pansharpened in ArcGIS Pro 2.6.0 using the Gram-Schmidt algorithm

283 and Pleiades sensor band weights to create a four-band (red, green, blue, and near infrared (NIR)) 0.5 m resolution multi-

284 spectral image. Quito's vegetated greenspace distribution was mapped using the NDVI applied to the NIR and red bands of

285 the pansharpened Pleiades satellite imagery (Fig. 3b):

286

287 $$NDVI = \frac{(NIR - Red)}{(NIR + Red)} \qquad (2)$$

288 Negative NDVI values correspond to areas lacking vegetation, whereas increasingly positive values represent healthy
289 vegetation (Tucker et al., 1981; Pettorelli et al., 2005). Bright blue roofs also displayed a high NDVI value and were masked
290 out using a simple 'blueness' index of values ≤ 0.2, which was derived through manual inspection of blue roofs:

292 $Blueness = 2 \times Blue - Red - Green$ (3)

294 Whilst global coverage and daily observation is possible with the paired constellation, Pleiades imagery is not routinely
295 acquired nor open access. Therefore, we also compared Pleiades NDVI values with those from an open access Sentinel-2
296 image acquired 6th February 2020 with the aim of testing their consistency, noting that whilst the spectral bands overlap, the
297 bandwidth of Pleiades is greater (Pleiades: red 590–710 nm, NIR 740–940 nm, Sentinel-2: red 649–680 nm, NIR 780–886
298 nm).

299 3.4.1 Disaster risk reduction (DRR) greenspace

300 Greenspaces potentially suitable for providing safe spaces and contributing towards disaster risk reduction were identified
301 using an EO-based workflow (Fig.3b) for areas within 800 m (accessible within a ~10-minute walk) (e.g. Dou and Zhan,
302 2011; Jeong et al., 2021) of populations in Quito's urban extent. The workflow identified greenspace: (1) that is vegetated,
303 (2) greater than 10 m from a road to exclude road verges; (3) with slope ≤4° to provide a suitable gradient for 'safe spaces'
304 (Kılcı et al., 2015; Liu et al., 2011); and (4) with a local height (≤2 m) to identify open ground and exclude raised vegetation
305 such as trees. Expansion and contraction buffers of 10 m were applied to connect adjacent patches of greenspace into
306 greenspace 'zones', which for example could represent multiple patches of classified greenspace within a park. All areas of
307 greenspace with a patch size ≥100 m^2 within these zones were summed and zones totalling ≥2000 m^2 of greenspace were
308 classified as 'potential DRR greenspace'. Space requirements in a disaster situation are dynamic; however, a 100 m^2 patch
309 size is recommended to accommodate two people with communal space (cooking, access, facilities etc) in a camp-style
310 settlement following guidelines in the Sphere Humanitarian Charter and Minimum Standards in Humanitarian Response
311 Handbook (Anhorn and Khazai, 2015; Sphere Association, 2018). Zones of 2000 m^2 approximate one quarter to one third of
312 a professional football pitch so could be expected to already exist as functional greenspaces (e.g. recreation parks) in an
313 urban environment. These spaces were evaluated alongside a list of safe spaces designated by DMQ for use in an earthquake
314 event (Metro Ecuador, 2019)(Table S3), in conjunction with population data projected to 2019 and socioeconomic
315 classification data (Instituto Geográfico Militar, 2019). These socioeconomic classes characterise a continuum of education,
316 income, and lifestyle factors into five classes, ranging from 'high' to 'low', where 'low' represents basic education and
317 limited household facilities such as rubbish collection and plumbing, whereas 'high' represents higher education, and houses
318 or apartments that are provisioned with state services (Instituto Geográfico Militar, 2019).

3.4.2 Greenspace capacity

Quito's 2019 population data (Instituto Geográfico Militar, 2019) were used to assess the population capacity of all DRR greenspace (3.4.1) in the event that they were to be used for accommodation following a disaster such as an earthquake. We assessed the capacity of two types of greenspaces: (1) DRR greenspace that overlapped with DMQ designated greenspaces, which included city parks and safe spaces (3.4.1), and (2) all DRR greenspaces identified in this study that were either designated or undesignated. These two scenarios therefore represent the DRR capacity based on current designations (1), compared to the potential maximum capacity (2). We considered two separate cases of populations within 800 m and 1600 m network buffers of each greenspace. For each scenario, we used a network analysis to assign population demand points to each greenspace based on their proximity, up to the maximum buffer distance. The network was constructed as a grid at 100 m resolution and considered population demand points also gridded at 100 m resolution, which were uniformly disaggregated from census polygons. The number of people that could be accommodated in each greenspace depends on the capacity of the space, and the population demand in the surrounding buffer. We considered capacities based on Sphere Association (2018) guidelines, which suggest an allocation of 45 m^2 per person (recommended amount per person accounting for communal facilities and infrastructure in an emergency shelter setting) and 3 m^2 per person (minimum living space per person). All demand within the buffers was allocated to the closest greenspaces, therefore excess demand was reported as overcapacity. We did not consider the possibility of people moving greater distances around the city to distribute the population demand more equally, which could occur following an initial disaster situation, or that only a fraction of the population would require access to refuge space in a disaster situation. Considering potential policy consideration, we also used a maximum capacitated coverage network analysis (e.g. Anhorn and Khazai, 2015) with the same datasets to find the 'top ten' DRR greenspaces in Quito based on a minimum space requirement of 3 m^2 per person.

4 Results

4.1 Urban growth

Our land cover classifications showed that the urban area of Quito expanded ~192 km^2 over the study period, more than doubling from 160±50 km^2 in 1986 to 352±47 km^2 in 2020 (Fig. 4, Table S4). Urban expansion was primarily aligned along-valley (north south) and eastward (Fig. 5a), into areas of previously scrub vegetation/bare and agricultural/grassland classes. The future urbanisation scenario of Bonilla-Bedoya et al. (2020b) covered an urban area of 1,232 km^2 (F-U), whereas the M-U scenario covered 705 km^2 (Fig. 4a), which was still double the observed 2020 urban area. Future urbanisation in the modelled scenarios was predominantly eastward, where lower density urbanisation interspersed with the scrub vegetation/bare ground class was already apparent in 2020 (Fig. 5). The area of woodland and agriculture/grassland classes also increased 1986–2020. A notable example of afforestation (4.8 km^2) was the park Metropolitano del Sur, which is located on the southeast of the city limit (Fig. 5a).

350

351
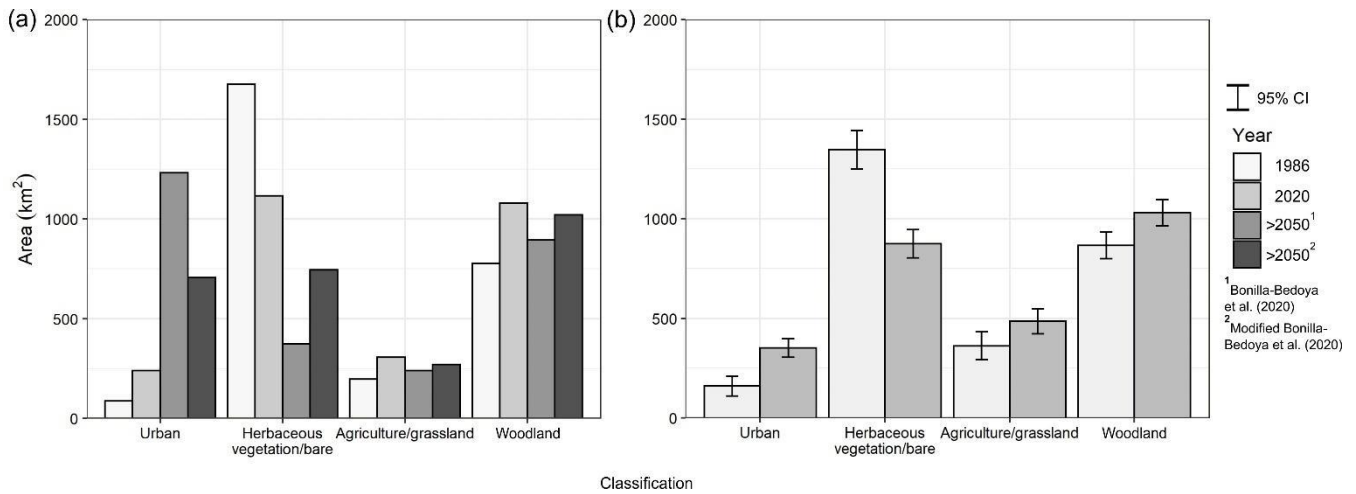
Figure 4: (a) Mapped land cover classification results for 1986 and 2020 alongside modelled future land cover from two scenarios[1, 2] using data from Bonilla-Bedoya et al. (2020). (b) Error-adjusted (e.g. Olofsson et al., 2013; Olofsson et al., 2014) land cover classification results from 1986 and 2020.

355

356

357

Figure 5: (a) 3D perspective showing urban growth 1986–2020 and land cover. (b) Quito's urban area in 2020 compared to modelled future urbanisation (F-U) (Bonilla-Bedoya et al., 2020) and a modified scenario (M-U). Background is a hillshaded SRTM DEM.
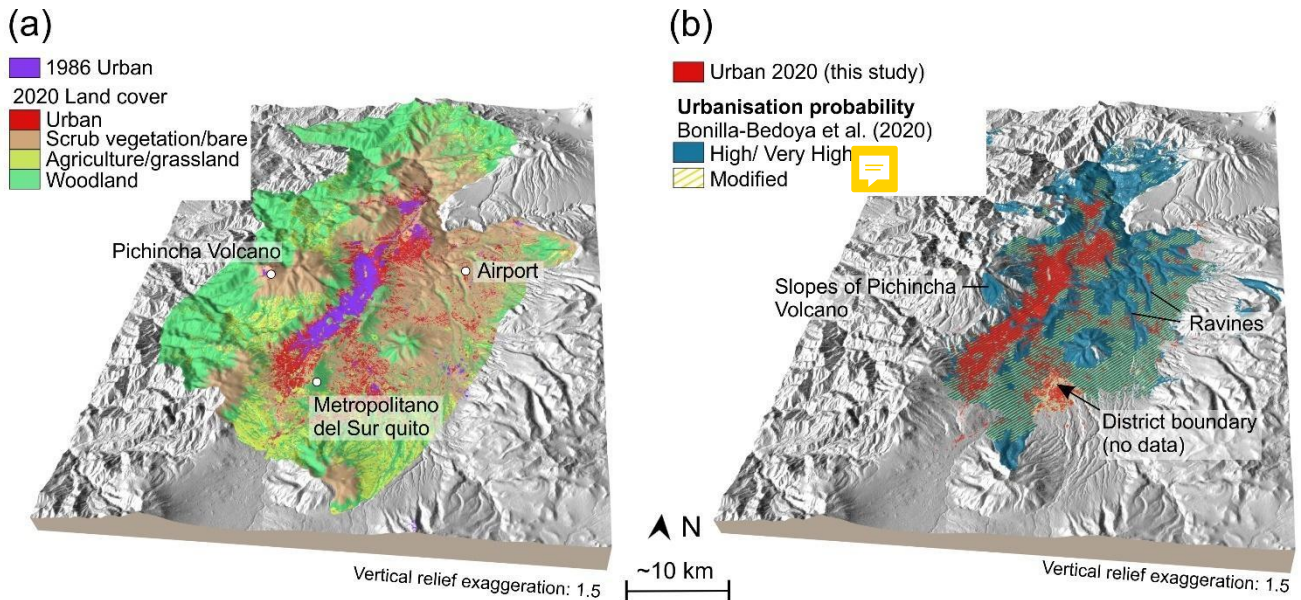
The median elevation of Quito's urban extent in 2020 (2,780 m) was similar to 1986 (2,810 m); however, the city covered a

broader elevation range in 2020, tending towards lower elevations (Fig. 6a), which was also apparent for the F-U and M-U

363 scenarios. The urban class displayed the smallest spread of values for topographic slope (Fig. 6b). Here, the median slope of

364 the urban class was ~5° in 1986 and 2020, however this increased to 11° and 7° in the F-U and M-U scenarios respectively,

365 in addition to a broader spread of slope values. Woodland featured the highest median slope of all land cover classes (~28°)

366 and a comparable median elevation to the urban class (~2700–2800 m).

367
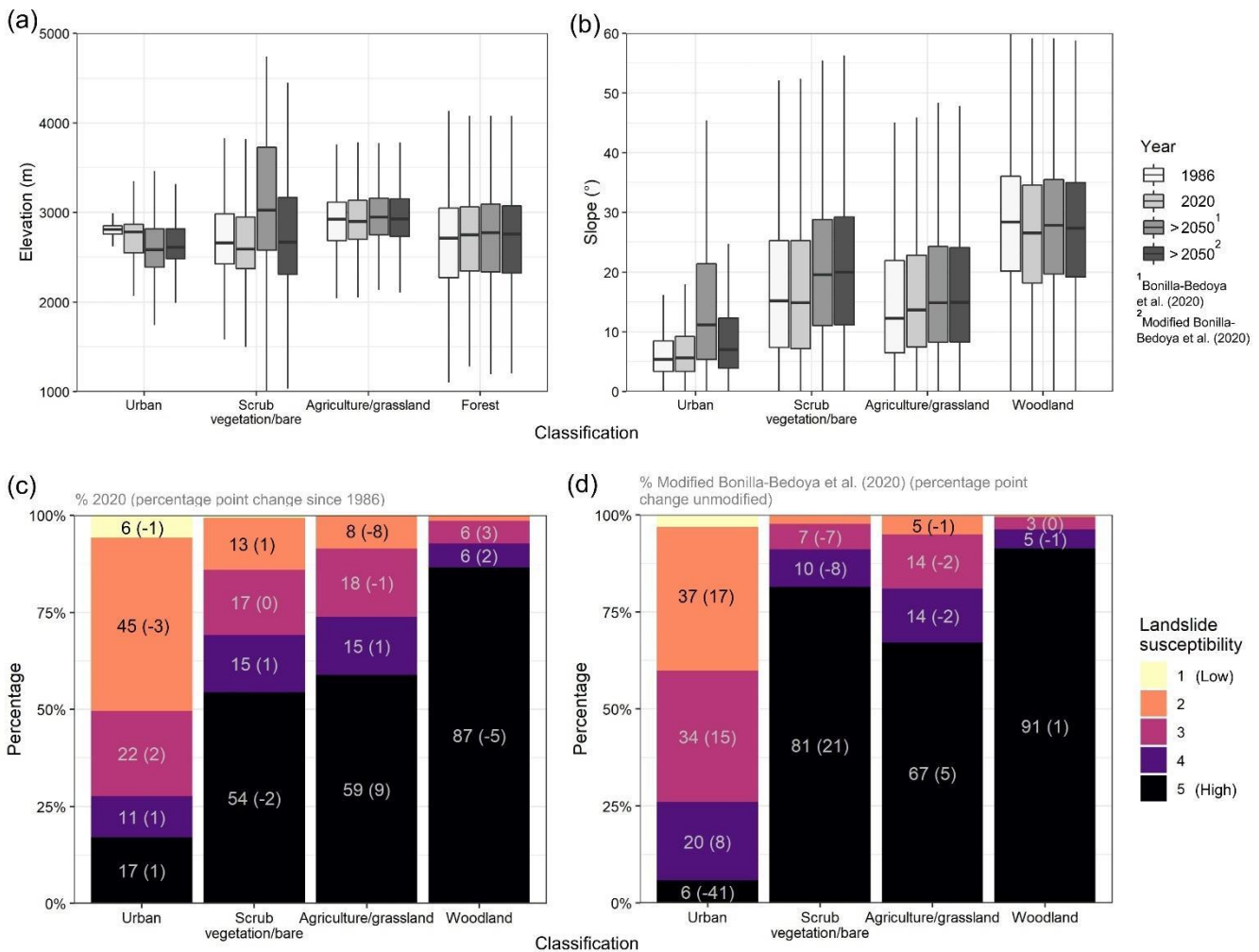
368

369 **Figure 6: Elevation (a) and slope (b) characteristics of the classified and modelled land cover scenarios. Boxes show the**
370 **interquartile range and the median (horizontal line). Lines show values within 1.5 times the interquartile range. Outliers are not**
371 **shown. (c) 2020 land cover intersections with landslide susceptibility and the percentage points change since 1986. (d) Future land**
372 **cover intersections with landslide susceptibility using modified urbanisation probability (M-U) of Bonilla-Bedoya et al. (2020, and**
373 **the difference compared to the unmodified scenario (F-U).**

4.2 Intersection with hazards

Landslides are one of the most common natural hazards in Quito (DMQ, 2018). We found good spatial association between observations of landslide events in Ecuador's Open Government database (2006–2017) and a landslide susceptibility model (Stanley and Kirschbaum, 2017) (Fig. S4). Of 1,321 recorded events, 82% (n = 1,089) fell within landslide susceptibility categories 3–5, of which 44% (n = 576) were in the highest category (5). Ten events were observed in the lowest category (1). We observed a small change in the landslide susceptibility of the urban class 1986–2020. Here, the urban area in the highest landslide susceptibility categories (4 and 5) increased by 2 percentage points 1986–2020 (Fig. 6c). The largest change was observed in the agriculture/grassland class, which featured a 9-percentage point increase in category 5 (high) landslide susceptibility. Woodland mostly occurred within the highest landslide susceptibility category 5 (87%) (Fig 6c). Regarding future urbanisation, the M-U scenario restricted future urbanisation in landslide susceptibility category 5, therefore the observed percentage of urban area in category 5 (6%) was notably lower than in the F-U scenario (47%), which did not enforce any restrictions.

Flood events in Quito that were recorded in Ecuador's Open Government database were evaluated alongside a TWI derived from the 10 m resolution Pleiades DEM. Median TWI values for all flood events (n = 1,274), clustered flood events where two or more events were located within 40 m of each other (n = 125), and a random sample (n = 10,000), were 13.3, 14.4, and 12.1 respectively (Fig. S6). Clustered flood events, which displayed the highest TWI, could correspond to areas of nuisance flooding since multiple events are located in close proximity (Kelleher and McPhillips, 2020). Two sample independent Welch t-tests (one-tailed) showed that the difference in TWI values between all flood events and clustered floods events were statistically significantly different from the random sample ($p < 0.05$). Therefore, the mean TWI value was observed to be larger in areas of flood locations compared to the random sample.

4.3 Greenspace

Quito includes multiple types of greenspace that provide ecological, social, and disaster risk reduction benefits (Fig. 1, 7). Within our AOI, 18.6 km^2 of potential DRR greenspace was identified, which covered 6% of the urban zone (Fig. 8). DMQ designated greenspace had an area of 36.9 km^2, of which 2.5 km^2 (7%) intersected with potential DRR greenspace. Similarly, DMQ designated safe spaces covered 17.3 km^2, of which 1.7 km^2 (10%) intersected with potential DRR greenspace. Comparing DRR greenspaces with hazard information revealed that 62% of DRR greenspace intersected with areas of high TWI values(>=14.4 (median value for clustered flood events - Section 4.2)), 10% intersected with areas of high (category 5) landslide susceptibility, and 6% intersected with both hazards (Fig. 8b).
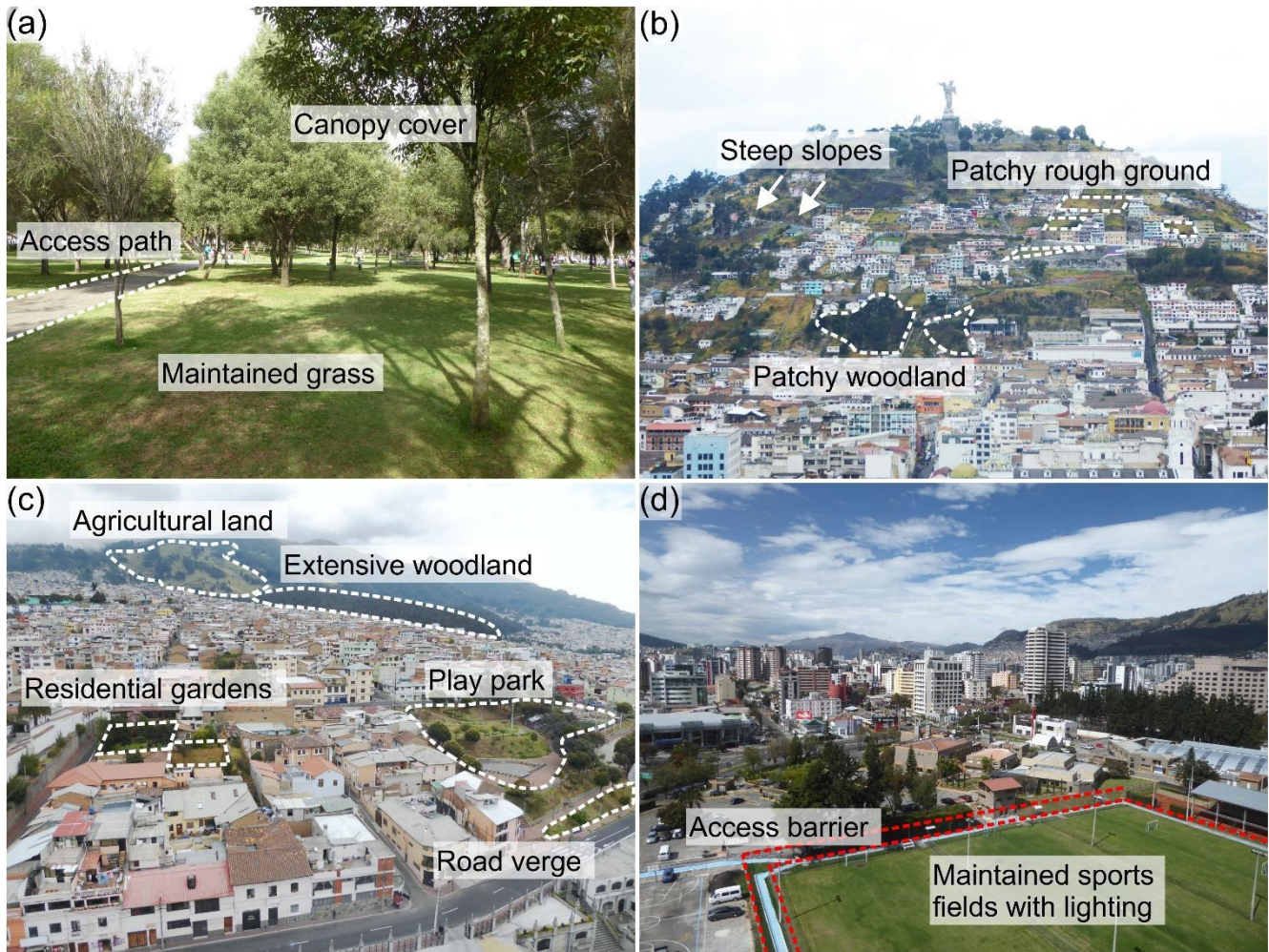
Figure 7: Examples of greenspace in Quito from photographs taken in October 2019 (a–d).

405
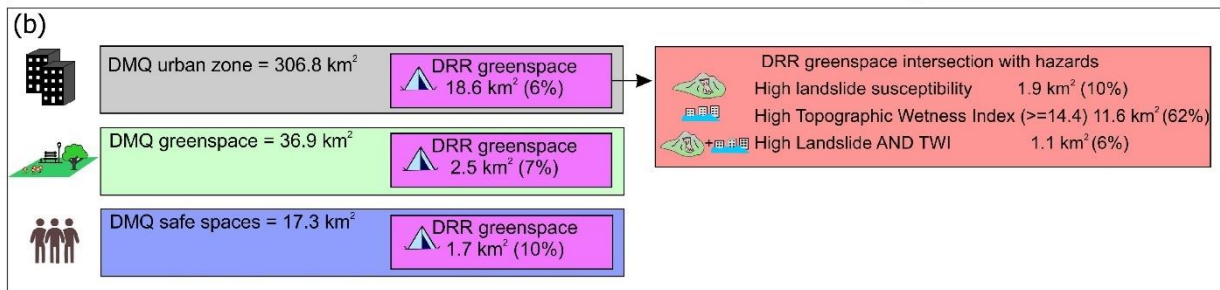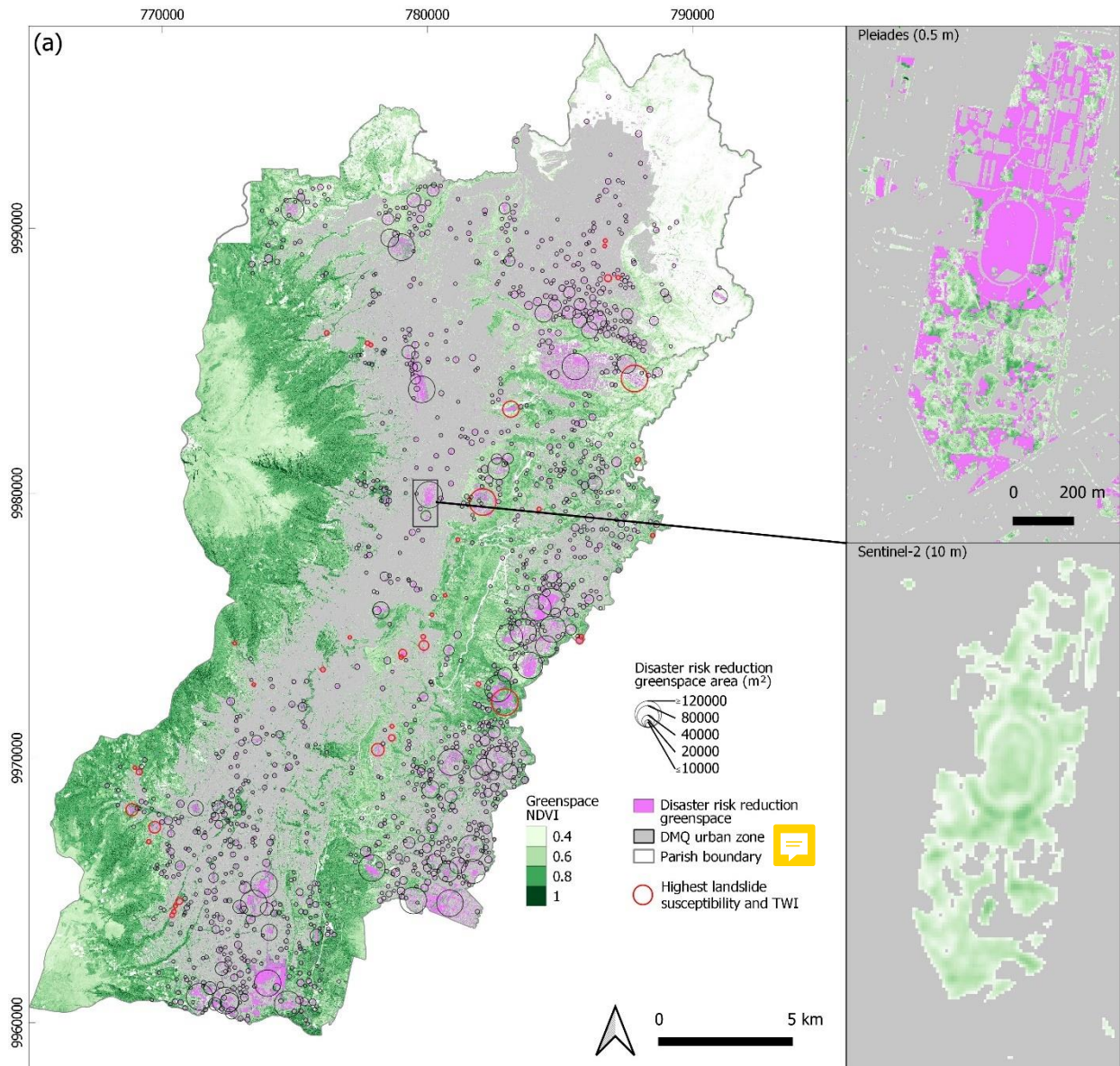
Figure 8: Greenspace mapped using the NDVI applied to Pleiades satellite imagery shown with classified potential DRR greenspace (black and red circles, pink shading). Red circles indicate DRR greenspace that intersects with landslide susceptibility class 5 (high) and a Topographic Wetness Index value of >=14.4 (median value for clustered flood events - Section 4.2). The inset of Carolina Park shows the similarity of Pleiades-derived greenspace compared to greenspace mapped using Sentinel-2 imagery. The Pleiades inset shows the distribution of potential DRR greenspace (pink) in Carolina Park. (b) Summary of greenspace availability and hazard intersections.

The association between population, socioeconomic classification (Instituto Geográfico Militar, 2019), and greenspace accessibility was investigated for greenspaces $\geq$2000 m^2. The number of people livsing within close proximity to designated greenspace was higher than for DRR greenspace (Fig. 9a). For example, 2.3 million (98%) of Quito's population were within 800 m of a designated greenspace, compared to 2.1 million for the DRR greenspace (88%). Distance to the nearest greenspace was greater for 'low' and 'medium low' socioeconomic classifications compared to 'high' and 'medium high' (Fig. 9b). Here, the difference in median values was greatest for designated greenspace (466 m), compared to our classification of DRR greenspace (80 m). The amount of designated greenspace per person was smaller for lower socioeconomic classifications, with a median of 3 m^2 per person for the 'low' classification compared to 8 m^2 for 'high'. However, the amount of DRR greenspace was greatest for lower socioeconomic classifications, with a median of 24 m^2 per person for 'low' compared to 4 m^2 for 'high' (Fig. 9c). This reflects lower population densities on the city margins (Fig. 9d) and the persistence of agricultural land and undeveloped ground in these areas following urbanisation.
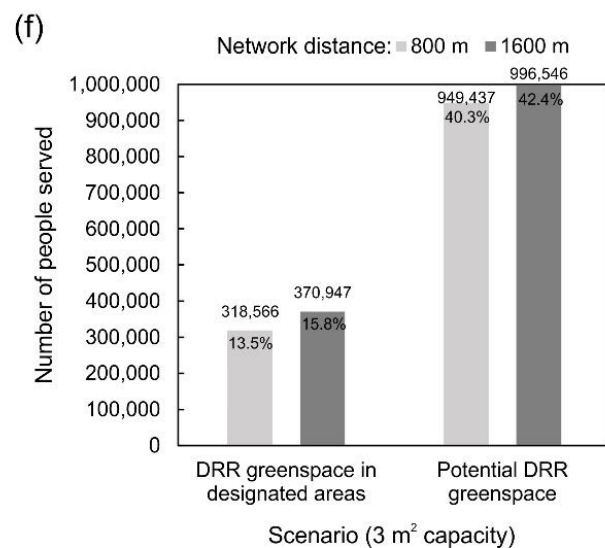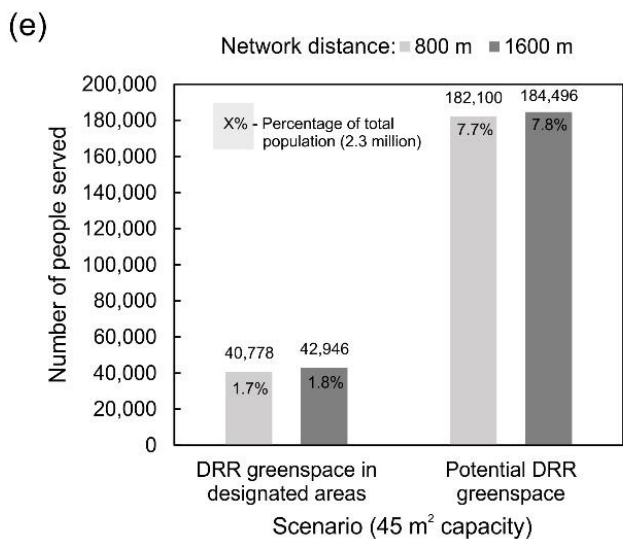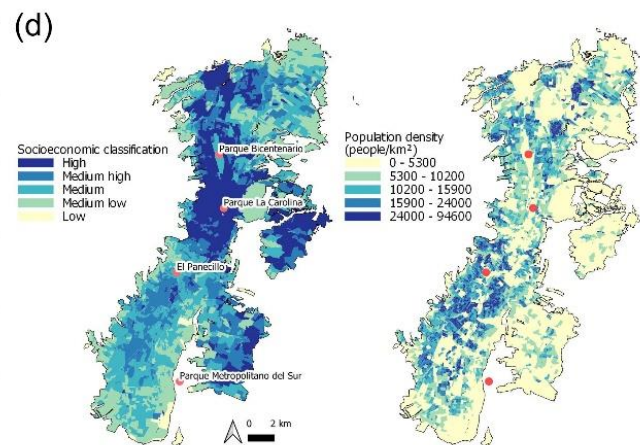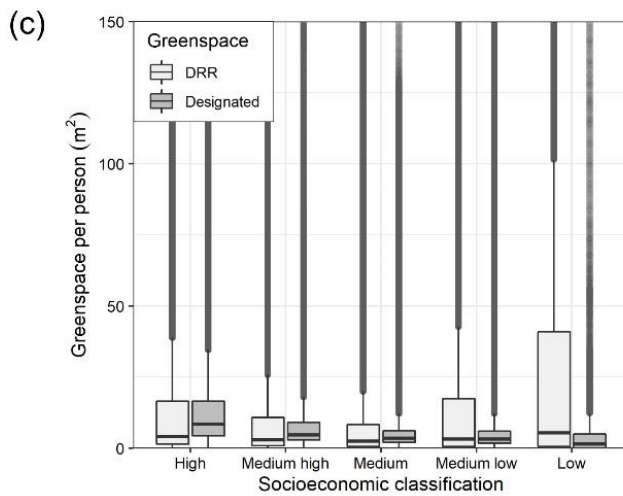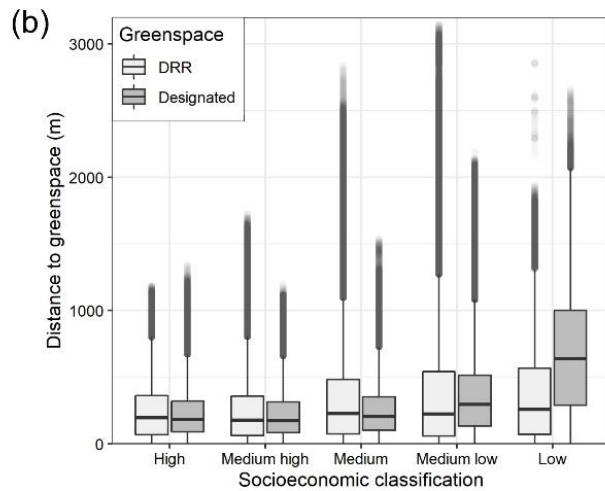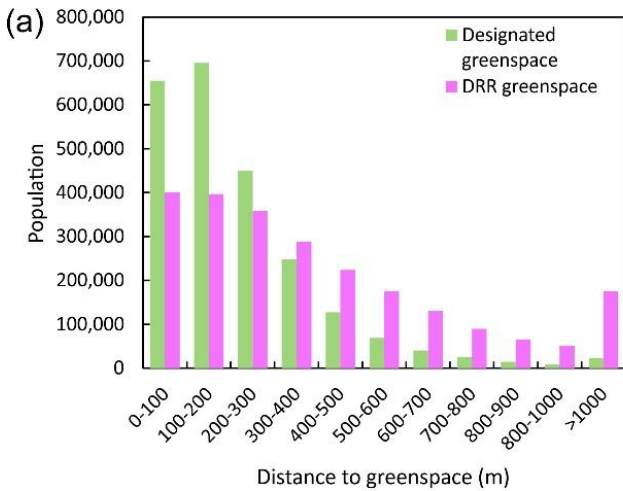
Figure 9: (a) Population proximity to designated and DRR greenspace. (b) Distance to the nearest greenspace for each socioeconomic classification. Boxes show the interquartile range and the median (horizontal line). Lines show values within 1.5 times the interquartile range. Outliers are shown as black markers with transparency. Outliers beyond the y-axis range (c) were excluded. (c) Greenspace per person within 800 m for each socioeconomic classification. (d) Spatial variation in socioeconomic classification and population density for Quito using data from Instituto Geográfico Militar (2019). (e) Number of people that could be accommodated in DRR greenspace based on an allocation of 45 m² per person capacity and (f) 3 m² per person capacity. (e-f) Show capacitated populations for a network distance of 800 m (light grey bars) and 1600 m (dark grey bars) from the greenspace centroid and for DRR greenspace in designated spaces compared to all potential DRR greenspace mapped in this study.

4.3.1 Greenspace capacity

We assessed the capacity of each space considering the surrounding population demand. For populations within 800 m, DRR greenspace in currently designated areas could accommodate 1.7% (40,778) of Quito's population (total 2.3 million) with an allocation of 45 m² per person, or 13.5% (318,556) with 3 m² per person (Fig. 9 e-f, 10a). Considering all potential DRR greenspace (Fig. 8a), these values are 7.7% and 40.3% respectively (Fig. 9e-f). The top ten DRR providing greenspaces are shown in Figure 10b and Figure 11. Eight of these spaces overlap fully or partially with currently designated greenspaces or safe spaces and two did not (Fig. 11). Of these 278 currently designated spaces, only 10 were not over capacity based on the population demand (Fig. 10b).
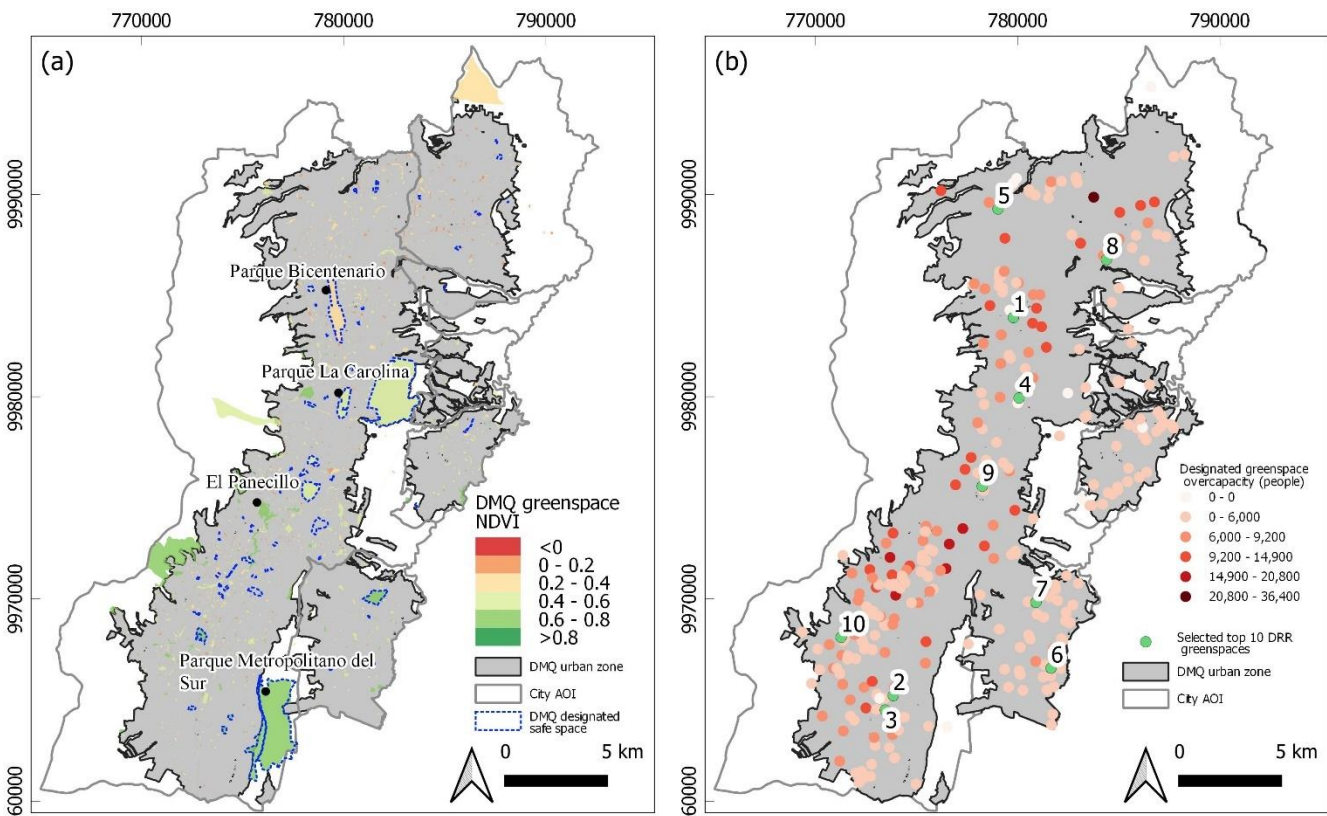
Figure 10: (a) Designated green areas and safe spaces (blue dashed polygons) from Open Government data and their mean NDVI extracted using Pleiades satellite data. (b) Overcapacity of DRR greenspace in currently designated greenspaces or safe spaces. Green markers show the top 10 DRR greenspaces based on a maximum capacitated coverage model.

Figure 11. Top ten ranked DRR greenspaces (red) and other nearby DRR greenspaces (pink).

5 Discussion

5.1 Urban growth and hazard intersections

Quito's historical urban expansion is largely aligned north-south, whereas future urban expansion is focussed to the north and east (Fig.5). Our study captures a period of land occupations starting in the 1980s including the settlement of Atucucho (Fig. 2b), which formed informally in 1988 (Testori, 2016). This occupation is visible in our land cover classification (Fig. 5a). The formation date is 2003 in Open Government data (Fig. 2b), which likely reflects its origins as an informal settlement. In this case, satellite imagery can capture the sprawl of a city, including occupations that may not be apparent in historical maps. However, image classification methods usually only capture 2D sprawl, and not vertical high-rise

457   developments or redevelopments that are important for measuring exposure to natural hazards (e.g. Amey et al., 2021).
458   Quito's past and projected urban growth has been studied by several authors in recent years (e.g. Bonilla-Bedoya et al.,
459   2020b; Salazar et al., 2020; Valencia et al., 2020). Cross-comparisons are complicated by the use of different study areas
460   since Quito's urban area now exceeds the designated metropolitan district boundary, which has prompted investigations to
461   create a new district area (Salazar et al., 2021). By comparing our urban classification (year 2020) to that of Bonilla-Bedoya
462   et al. (2020) (year 2016) within the same area of interest, we find urban areas of 213 km² and 210 km² respectively, which
463   indicates classification consistency using EO data despite different methodological approaches.

464

465   Limited urban expansion to the east of Quito on the steep slopes of Pichincha volcano suggests that a programme of
466   protection to avoid encroachment is working (Vidal et al. 2015). However, several of these areas or their vicinities are
467   inhabited because of previous land invasion dynamics that affected the peripheral green belt. They can be characterised from
468   a spatial and socioeconomic approach as a homogeneous space, in which the less economically favoured classes experience
469   greater possibilities of isolation from other social groups (Bonilla-Bedoya et al., 2020a). Further limiting eastward urban
470   growth reduces the ashfall and lahar hazard in the event of an eruption (Fig. 2c) and the hazard posed by landslides (Fig. 2d).
471   Additionally, the predominantly woodland slopes east of Quito (Fig. 5a) featured the highest landslide susceptibility scores
472   (87% of woodland is in class 5 (High) (Fig. 6c)) and are therefore a valuable target for protection against urbanisation. Our
473   observed decreasing elevation trend of Quito's urban area (Fig. 6a) reflects north-south and eastward expansion into lower
474   lying flatter areas, such that at a city-scale, Quito's landslide susceptibility did not notably increase 1986–2020 (Fig. 6c).
475   These areas are also the location of projected future expansion (Bonilla-Bedoya et al., 2020b; Salazar et al., 2020; Valencia
476   et al., 2020), predominantly through conversion of scrub vegetation and bare ground (Fig. 5a). Notable ravines exist in these
477   areas, therefore risk-informed planning to reduce encroachment on steep slopes, which was reflected in our M-U future
478   urban scenario, is desirable to minimise landslide risk to future developments. These areas are also likely to be most
479   susceptible to multi-hazards such as rainfall triggered lahar remobilisation or landslides, and flood and earthquake triggered
480   landslides (Gill and Malamud, 2017). Similarly, the filling of ravines from the seventeenth century onwards restricts the
481   drainage capacity during intensive rainfall and increases flood risk (Aragundi et al., 2016), therefore, incorporating
482   additional DRR greenspaces here to attenuate runoff and store water could be beneficial.

483

484   While risk-informed urbanisation can mitigate some hazards such as landslides, an intensive earthquake hazard exists in
485   Quito (Fig. S1), such that urban risk reduction requires building resilience at community to city-wide levels (Alvarado et al.,
486   2014; Valcárcel et al., 2017). A key element of resilience is the access to 'safe spaces' following an earthquake event where
487   communities can avoid damaged buildings and infrastructure and receive emergency aid (Sphere Association, 2018). These
488   spaces are increasingly viewed within a broader network of benefits to society and ecosystems (e.g. Fig.1a), and framed
489   within Eco-DRR strategies (UNDRR, 2020). We therefore evaluated greenspaces in Quito that could offer DRR capabilities
490   by both considering existing designated greenspaces and assessing other non-designated greenspaces.

5.2 Greenspace

Our study was designed to identify the basic requirements for sites that could be designated or developed as DRR greenspace using an earth-observation based methodology that could be adapted and applied to other cities. This is timely since greenspace is becoming increasingly desirable to improve environment quality, contribute to addressing climate breakdown, and greenspace within Eco-DRR strategies can simultaneously mitigate against multiple hazards (Onuma and Tsuge, 2018; McVittie et al., 2018; Sudmeier-Rieux et al., 2021). Our DRR greenspace primarily addresses the basic requirements of people-space and amenable topography for medium- to long-term accommodation requirements, such as following a major earthquake. Examples are shown in Figure 12 for areas in central Quito and on the periphery. Regarding urban risk, green space in Quito has been thought of from the perspective of threat. For example, interventions have been developed on the slopes of Pichincha from a logic of risk mitigation (Vidal et al., 2015). Recently, after the 2016 Ecuador earthquake, green and open spaces were incorporated throughout the city as safe points in case of evacuation (Rebotier, 2016) (Fig. 10a).
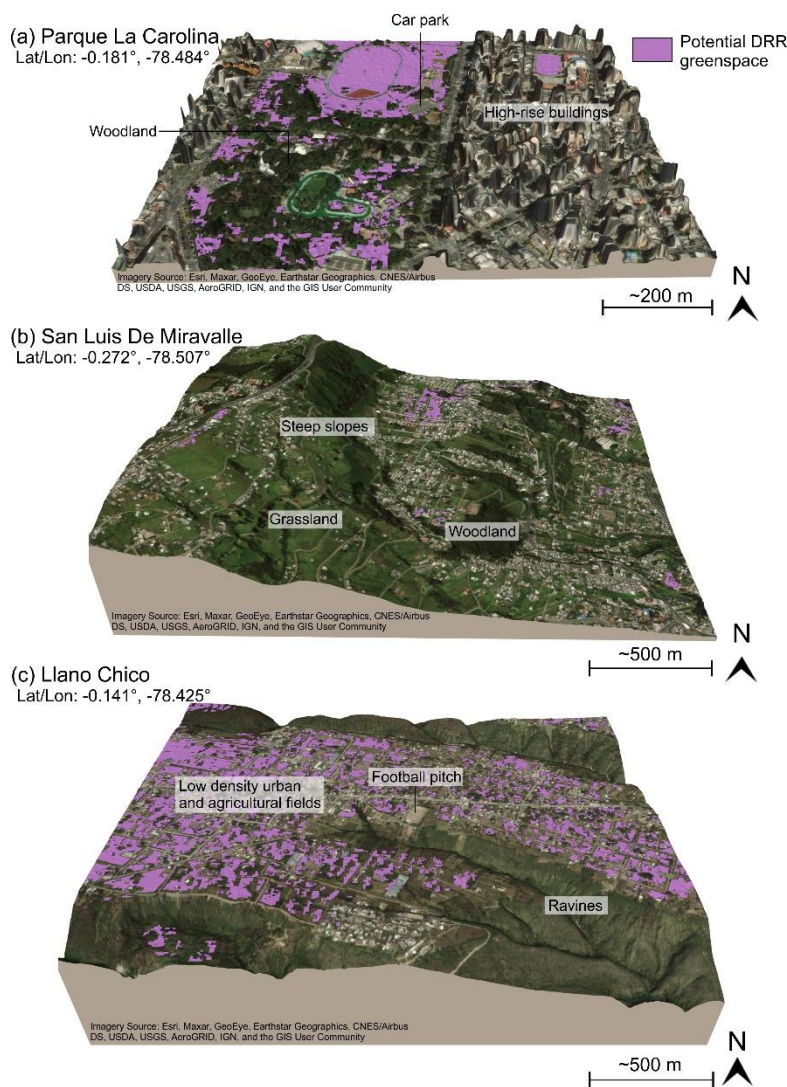
Figure 12: 3D perspective showing examples of potential DRR greenspace identified in Quito. (a) Parque La Carolina is in central Quito amongst commercial high-rise buildings. (b) San Luis De Miravalle is located on the southeast of Quito and is characterised by lower density urban development and steep slopes. (c) Llano Chico is in the east of Quito with low density urban development mixed with agricultural land that is bounded by steep ravines.

We found that 7% (2.5 km^2) of the DMQ designated greenspace was identified as potential DRR greenspace. Similarly, 10% (1.7 km^2) of the DMQ designated safe spaces intersected with our classified DRR greenspace (Fig. 8, 10a). The total area of potential DRR greenspace within Quito was 18.6 km^2, therefore large potential exists to incorporate new greenspaces into a DRR framework, especially in the south and east of the city, which are locations of projected future expansion and where urban expansion and population densities are lower (Fig. 5b, 9d). New designation of greenspaces could address some of the imbalance between greenspace access since 98% (~2.3 million) of Quito's population were within 800 m of a designated greenspace, compared to 2.1 million for the DRR greenspace (88%) (Fig. 9a). Lower socioeconomic classifications had a

greater distance to travel to the nearest designated greenspace, and a lower greenspace area per person overall (Fig. 9b, c), which was also observed by Cuvi et al. (2021), noting that informal developments have less access to larger designated parks. We found a median designated greenspace of 3 m^2 per person for the 'low' socioeconomic classification. However, the availability of potential DRR greenspace to these same communities (median of 24 m^2) shows that additional designations could help address the imbalance. This is also aligned with Quito's Vision 2040 document to increase greenspace in urban areas to ~9 m² per person (DMQ, 2018). Critical to addressing these inequalities is to ensure that all formal and informal settlements are reflected in socioeconomic statistics and included in official maps.

Although we found high accessibility of greenspace within 800 m of populations, the capacity to serve surrounding populations for emergency refuge was 1.7% considering the recommended space allocation of 45 m^2 per person (Fig. 9a)(Sphere Association, 2018). Incorporating all additional spaces that are DRR suitable could increase this to 8 %, or 40% using a minimum living allocation of 3 m^2 per person (Sphere Association, 2018). A network analysis producing a ranked top ten DRR greenspaces (Fig. 11) showed that eight intersected with currently designated greenspaces or safe spaces and two did not. These two spaces could be investigated for negotiating formal access to these spaces for use in an emergency, such as the golf club forming Site 5 (Fig. 11e).

We focus on greenspace as an emergency refuge; however, these spaces can also contribute to mitigating hazards both through physical processes such as water retention or slope stabilisation (Phillips and Marden, 2005; Maragno et al., 2018; Sandholz et al., 2018), and also by their existence in places that would be hazardous if urbanised. We found that of the potential DRR greenspace identified in Quito, 62% intersected with TWI values indicative of potential flooding (section 4.2), 10% with areas of high landslide susceptibility, and 6% with both hazards (Fig. 8 – red circles). Therefore, there is potential to mitigate future risk by maintaining greenspace and therefore avoiding development in potentially hazardous areas, and incorporating additional DRR greenspaces that are not exposed to hazards for use as refuges.

5.3 Future work

Our study has provided a city-wide assessment of Quito's historical and future growth projections, and the potential role of greenspace in reducing disaster risk. The first-pass analysis of greenspace suitable for DRR could be used for local community-scale evaluation and stakeholder engagement to deliver improved resilience for the city. Subsequently, the methodology could be expanded to define a continuum of greenspace suitability for DRR by incorporating other important factors including site specific suitability trade-offs such as land value, ownership, and access to water, electricity, and hospitals (Anhorn and Khazai, 2015; Hosseini et al., 2016). Similarly, we focussed on greenspaces since these spaces are most likely to be accessible and they provide multiple benefits; however, concreted grey spaces such as commercial car parks could also serve a role in providing safe spaces for DRR, particularly if a disaster event occurred during work hours.

547 Methodological improvements could include multi-temporal and potentially higher resolution datasets, for example landslide

548 susceptibility information that reflects changing land cover and therefore an evolving hazard (Emberson et al., 2020).

549

550 Use of EO-based datasets broadens the applicability of our methods to other cities. Whilst coarser resolution satellite

551 imagery could still delineate the types of greenspaces relevant to DRR (e.g. Fig. 8 inset), we relied on a high resolution

552 Pleiades DEM to provide topographic relief information on the greenspace DRR suitability. Global 30 m resolution DEMs

553 could likely substitute this in some cases, though not in densely built urban environment where flat open greenspaces are

554 interspaced with tall buildings and trees for example (Fig. 12a), which cannot be resolved in 30 m elevation models.

6 Conclusion

556 In this study, we used a combination of satellite data analysis and secondary datasets to quantify Quito's historical growth,

557 future intersection with hazards, and distribution of greenspace within the city. Quito's historical growth (~192 km^2 1986 to

558 2020) was primarily on flatter, former agricultural land, hence there was limited encroachment towards hazards of Pichincha

559 volcano and areas of higher landslide susceptibility. However, our work shows that future urbanisation projections suggest

560 an increasing intersection between urban areas and areas of high landslide susceptibility, which requires risk-informed

561 planning to mitigate. General accessibility of greenspaces is high, with 98% (2.3 million) of Quito's population within 800 m

562 of a designated greenspace and 88% (2.1 million) for the DRR greenspace classification. However, within 800 m, the

563 capacity of currently designated greenspaces and safe spaces would only fulfil 2% of Quito's population. Over 40% could be

564 accommodated by incorporating new DRR greenspaces identified in this study. We also found a disparity between access to

565 greenspaces across socio-economic classifications, with low-medium groups having less access to designated greenspace. In

566 some cases, these low-medium groups have the greatest opportunity for future designation of DRR greenspace due to their

567 location on the city periphery in areas of lower population density. Our workflow uses satellite data to provide a first-pass

568 evaluation of DRR greenspace potential and could therefore be adapted for application in other developing cities. The results

569 provide the foundation to evaluate these spaces with stakeholders at community to city-wide scales, since promoting

570 equitable access to greenspaces, communicating their multiple benefits, and considering their use to restrict development in

571 hazardous areas will be key to sustainable, risk-informed urban growth.

Data availability

573 The data used to support the findings and results of this study are available in the supplementary information and in the

574 Zenodo repository https://doi.org/10.5281/zenodo.5881876. Pleiades imagery data were provided through the CEOS Seismic

575 Hazard Demonstrator and are restricted by license.

Author contribution

All authors have read and agreed to the published version of the manuscript. CSW, ES, MAV, JRE, and SKE designed the concept. JRE, CZ, SB-B, PC, DFO provided access to datasets. CSW performed the analysis and prepared the figures. CSW wrote the manuscript with input from all authors.

Competing interests

The authors declare that they have no conflict of interest.

Financial support

This research has been supported the UK Research and Innovation (UKRI) Global Challenges Research Fund (GCRF) Urban Disaster Risk Hub (NE/S009000/1) (Tomorrow's Cities), a NERC Innovation award (grant number NE/S013911/1). and COMET. COMET is the NERC Centre for the Observation and Modelling of Earthquakes, Volcanoes and Tectonics, a partnership between UK Universities and the British Geological Survey. John Elliott is supported by a Royal Society University Research fellowship (UF150282), Susanna Ebmeier is supported by a NERC Independent Research Fellowship (NE/R015546/1).

Acknowledgments

The Committee on Earth Observation Satellites (CEOS) and Centre National d'Etudes Spatiales (CNES) are thanked for providing access to the Pleiades satellite imagery used in this study. Pleiades images made available by CNES in the framework of the CEOS Working Group for Disasters. © CNES (2018, 2019, 2020), and Airbus DS, all rights reserved. Commercial uses forbidden.

References

Airbus Defence and Space: Pléiades Imagery User Guide. [Accessed 29th October 2019] Available from: https://www.intelligence-airbusds.com/en/8718-user-guides, 2012.

Allan, P., Bryant, M., Wirsching, C., Garcia, D., and Teresa Rodriguez, M.: The Influence of Urban Morphology on the Resilience of Cities Following an Earthquake, Journal of Urban Design, 18, 242-262, 10.1080/13574809.2013.772881, 2013.

Altieri, M. A., Companioni, N., Cañizares, K., Murphy, C., Rosset, P., Bourque, M., and Nicholls, C. I.: The greening of the "barrios": Urban agriculture for food security in Cuba, Agriculture and Human Values, 16, 131-140, 10.1023/A:1007545304561, 1999.

602 Alvarado, A., Audin, L., Nocquet, J. M., Lagreulet, S., Segovia, M., Font, Y., Lamarque, G., Yepes, H., Mothes, P.,
603 Rolandone, F., Jarrín, P., and Quidelleur, X.: Active tectonics in Quito, Ecuador, assessed by geomorphological studies, GPS
604 data, and crustal seismicity, 33, 67-83, 10.1002/2012tc003224, 2014.

605 Amey, R. M. J., Elliott, J. R., Hussain, E., Walker, R., Pagani, M., Silva, V., Abdrakhmatov, K. E., and Watson, C. S.:
606 Significant Seismic Risk Potential from Buried Faults Beneath Almaty City, Kazakhstan, revealed from high-resolution
607 satellite DEMs, Earth and Space Science, https://doi.org/10.1029/2021EA001664, 2021.

608 Anhorn, J., and Khazai, B.: Open space suitability analysis for emergency shelter after an earthquake, Nat. Hazards Earth
609 Syst. Sci., 15, 789-803, 10.5194/nhess-15-789-2015, 2015.

610 Aragundi, S. M., Mena, A. P., and Zamora, J. J.: Historical Urban Landscape as a Descriptive Feature for Risk Assessment:
611 the 'Quebradas' of Quito, FICUP. An International Conference on Urban Physics, Quito – Galápagos, Ecuador, 2016.

612 Aronson, M. F., Lepczyk, C. A., Evans, K. L., Goddard, M. A., Lerman, S. B., MacIvor, J. S., Nilon, C. H., and Vargo, T.:
613 Biodiversity in the city: key challenges for urban green space management, Frontiers in Ecology and the Environment, 15,
614 189-196, https://doi.org/10.1002/fee.1480, 2017.

615 Baker, J. L.: Climate Change, Disaster Risk, and the Urban Poor, Climate Change, Disaster Risk, and the Urban Poor, 2012.

616 Bauwelinck, M., Casas, L., Nawrot, T. S., Nemery, B., Trabelsi, S., Thomas, I., Aerts, R., Lefebvre, W., Vanpoucke, C., Van
617 Nieuwenhuyse, A., Deboosere, P., and Vandenheede, H.: Residing in urban areas with higher green space is associated with
618 lower mortality risk: A census-based cohort study with ten years of follow-up, Environment International, 148, 106365,
619 https://doi.org/10.1016/j.envint.2020.106365, 2021.

620 Beauval, C., Mariniere, J., Yepes, H., Audin, L., Nocquet, J. M., Alvarado, A., Baize, S., Aguilar, J., Singaucho, J., and
621 Jomard, H.: A New Seismic Hazard Model for Ecuador, Bulletin of the Seismological Society of America, 108,
622 10.1785/0120170259, 2018.

623 Benedict, M., and MacMahon, E.: Green Infrastructure: Smart Conservation for the 21st Century, 2002.

624 Beven, K. J., and Kirkby, M. J.: A physically based, variable contributing area model of basin hydrology / Un modèle à base
625 physique de zone d'appel variable de l'hydrologie du bassin versant, Hydrological Sciences Bulletin, 24, 43-69,
626 10.1080/02626667909491834, 1979.

627 Bonilla-Bedoya, S., Estrella, A., Vaca Yánez, A., and Herrera, M. Á.: Urban socio-ecological dynamics: applying the urban-
628 rural gradient approach in a high Andean city, Landscape Research, 45, 327-345, 10.1080/01426397.2019.1641589, 2020a.

629 Bonilla-Bedoya, S., Mora, A., Vaca, A., Estrella, A., and Herrera, M. Á.: Modelling the relationship between urban
630 expansion processes and urban forest characteristics: An application to the Metropolitan District of Quito, Computers,
631 Environment and Urban Systems, 79, 101420, https://doi.org/10.1016/j.compenvurbsys.2019.101420, 2020b.

632 Borland, J.: Small parks, big designs: reconstructed Tokyo's new green spaces, 1923–1931, Urban History, 47, 106-125,
633 10.1017/S0963926819000567, 2020.

634 Boulton, C., Dedekorkut-Howes, A., and Byrne, J.: Factors shaping urban greenspace provision: A systematic review of the
635 literature, Landscape and Urban Planning, 178, 82-101, https://doi.org/10.1016/j.landurbplan.2018.05.029, 2018.

636 Bryant, M., and Allan, P.: Open space innovation in earthquake affected cities, in: Approaches to Disaster Management -
637 Examining the Implications of Hazards, Emergencies and Disasters, edited by: (ed.)., J. P. T., In-Tech, 2013.

638 Cardona, O., Aalst, M., Birkmann, J., Fordham, M., McGregor, G., Perez, R., Pulwarty, R., Schipper, L., and Sinh, B.:
639 Determinants of risk: Exposure and vulnerability, in managing the risks of extreme events and disasters to advance climate
640 change adaptation, 65-108 pp., 2012.

641 Carmin, J., and Anguelovski, I.: Planning Climate Resilient Cities: Early Lessons from Early Adapters, 2009.

642 Carrión, F., and Erazo Espinosa, J.: La forma urbana de Quito: una historia de centros y periferias, Bulletin de l'Institut
643 français d'études andines, 503-522, 2012.

644 Castelo, C. A. J., D´Howitt, M. C., Almeida, O. P., and Toulkeridis, T.: Comparative Determination of the Probability of
645 Landslide Ocurrences and Susceptibility in Central Quito, Ecuador, 2018 International Conference on eDemocracy &
646 eGovernment (ICEDEG), 2018, 136-143,

647 Chatelain, J. L., Tucker, B., Guillier, B., Kaneko, F., Yepes, H., Fernandez, J., Valverde, J., Hoefer, G., Souris, M., Dupérier,
648 E., Yamada, T., Bustamante, G., and Villacis, C.: Earthquake risk management pilot project in Quito, Ecuador, GeoJournal,
649 49, 185-196, 10.1023/A:1007079403225, 1999.

650 Colding, J., and Barthel, S.: The potential of 'Urban Green Commons' in the resilience building of cities, Ecological
651 Economics, 86, 156-166, https://doi.org/10.1016/j.ecolecon.2012.10.016, 2013.

652 Cuvi, N., and Vélez, L. C. G.: Los Parques Urbanos de Quito: Distribución, Accesibilidad y Segregación Espacial,
653 Environmental Science, 10, 2021.

654 De Sherbinin, A., Schiller, A., and Pulsipher, A.: The vulnerability of global cities to climate hazards, Environment and
655 Urbanization, 19, 39-64, 10.1177/0956247807076725, 2007.

656 Deng, J., Huang, Y., Chen, B., Tong, C., Liu, P., Wang, H., and Hong, Y.: A Methodology to Monitor Urban Expansion and
657 Green Space Change Using a Time Series of Multi-Sensor SPOT and Sentinel-2A Images, Remote Sensing, 11, 1230, 2019.

658 DMQ: Visión de Quito 2040 y su Nuevo Modelo de Ciudad, 2018.

659 Domínguez-Castro, F., García-Herrera, R., and Vicente-Serrano, S. M.: Wet and dry extremes in Quito (Ecuador) since the
660 17th century, International Journal of Climatology, 38, 2006-2014, 10.1002/joc.5312, 2018.

661 Dou, K., and Zhan, Q.: Accessibility analysis of urban emergency shelters: Comparing gravity model and space syntax, 2011
662 International Conference on Remote Sensing, Environment and Transportation Engineering, 2011, 5681-5684,

663 Emberson, R., Kirschbaum, D., and Stanley, T.: New global characterisation of landslide exposure, Nat. Hazards Earth Syst.
664 Sci., 20, 3413-3424, 10.5194/nhess-20-3413-2020, 2020.

665 Escobedo, F. J., and Nowak, D. J.: Spatial heterogeneity and air pollution removal by an urban forest, Landscape and Urban
666 Planning, 90, 102-110, https://doi.org/10.1016/j.landurbplan.2008.10.021, 2009.

667 Estrella, M., and Saalismaa, N.: Ecosystem-based disaster risk reduction (Eco-DRR): An overview, The role of ecosystems
668 in disaster risk reduction, edited by: Renaud, F. G., Sudmeier-Rieux, K., and Estrella, M., United Nations University Press,
669 2013.

670 Faivre, N., Sgobbi, A., Happaerts, S., Raynal, J., and Schmidt, L.: Translating the Sendai Framework into action: The EU
671 approach to ecosystem-based disaster risk reduction, International Journal of Disaster Risk Reduction, 32, 4-10,
672 https://doi.org/10.1016/j.ijdrr.2017.12.015, 2018.

673 Farr, T. G., Rosen, P. A., Caro, E., Crippen, R., Duren, R., Hensley, S., Kobrick, M., Paller, M., Rodriguez, E., Roth, L.,
674 Seal, D., Shaffer, S., Shimada, J., Umland, J., Werner, M., Oskin, M., Burbank, D., and Alsdorf, D.: The Shuttle Radar
675 Topography Mission, Reviews of Geophysics, 45, 10.1029/2005RG000183, 2007.

676 Fenger, J.: Urban air quality, Atmospheric Environment, 33, 4877-4900, https://doi.org/10.1016/S1352-2310(99)00290-3,
677 1999.

678 Flörke, M., Schneider, C., and McDonald, R. I.: Water competition between cities and agriculture driven by climate change
679 and urban growth, Nature Sustainability, 1, 51-58, 10.1038/s41893-017-0006-8, 2018.

680 Fuller, R., Groom, G., and Jones, A.: The land-cover map of great Britain: an automated classification of landsat thematic
681 mapper data, Photogrammetric Engineering and Remote Sensing, 60, 553-562, 1994.

682 García-Lamarca, M., Connolly, J., and Anguelovski, I.: Green gentrification and displacement in Barcelona, in: Housing
683 Displacement, Routledge, 156-170, 2020.

684 Georganos, S., Grippa, T., Vanhuysse, S., Lennert, M., Shimoni, M., and Wolff, E.: Very High Resolution Object-Based
685 Land Use–Land Cover Urban Classification Using Extreme Gradient Boosting, IEEE Geoscience and Remote Sensing
686 Letters, 15, 607-611, 10.1109/LGRS.2018.2803259, 2018.

687 Gill, J. C., and Malamud, B. D.: Anthropogenic processes, natural hazards, and interactions in a multi-hazard framework,
688 Earth-Science Reviews, 166, 246-269, https://doi.org/10.1016/j.earscirev.2017.01.002, 2017.

689 Gill, J. C., Hussain, E., and Malamud, B. D.: Workshop Report: Multi-Hazard Risk Scenarios for Tomorrow's Cities.
690 [Accessed 18th May 2021]. Available from: https://tomorrowscities.org/workshop-report-multi-hazard-risk-scenarios-
691 tomorrows-cities, 2021.

692 Godfray, H. C. J., Beddington, J. R., Crute, I. R., Haddad, L., Lawrence, D., Muir, J. F., Pretty, J., Robinson, S., Thomas, S.
693 M., and Toulmin, C.: Food Security: The Challenge of Feeding 9 Billion People, Science, 327, 812-818,
694 10.1126/science.1185383, 2010.

695 Gonzalez, C. G.: Seasons of Resistance: Sustainable Agriculture and Food Security in Cuba, Tulane Environmental Law
696 Journal, 16, 685-732, 2003.

697 Gorelick, N., Hancher, M., Dixon, M., Ilyushchenko, S., Thau, D., and Moore, R.: Google Earth Engine: Planetary-scale
698 geospatial analysis for everyone, Remote Sensing of Environment, 202, 18-27, https://doi.org/10.1016/j.rse.2017.06.031,
699 2017.

700 Gregory McPherson, E.: Accounting for benefits and costs of urban greenspace, Landscape and Urban Planning, 22, 41-51,
701 https://doi.org/10.1016/0169-2046(92)90006-L, 1992.

702 Hall, M. L., Samaniego, P., Le Pennec, J. L., and Johnson, J. B.: Ecuadorian Andes volcanism: A review of Late Pliocene to
703 present   activity,   Journal   of   Volcanology   and   Geothermal   Research,   176,   1-6,
704 https://doi.org/10.1016/j.jvolgeores.2008.06.012, 2008.

705 Hastenrath, S.: Annual cycle of upper air circulation and convective activity over the tropical Americas, Journal of
706 Geophysical Research: Atmospheres, 102, 4267-4274, https://doi.org/10.1029/96JD03122, 1997.

707 Hoekstra, A. Y., Buurman, J., and van Ginkel, K. C. H.: Urban water security: A review, Environ. Res. Lett., 13, 053002,
708 10.1088/1748-9326/aaba52, 2018.

709 Hosseini, S. A., de la Fuente, A., and Pons, O.: Multicriteria decision-making method for sustainable site location of post-
710 disaster temporary housing in urban areas, Journal of Construction Engineering and Management, 142, 04016036, 2016.

711 IG-EPN, IGM, IRD.: Mapa de Peligros Volcánicos Potenciales del Volcán Guagua Pichincha 3ra. Edición, Quito - Ecuador.
712 Availalble online: https://www.igepn.edu.ec/ggp-mapa-de-peligros/file (accessed 10 December 2020). 2019.

713 Inglada, J., and Christophe, E.: The Orfeo Toolbox remote sensing image processing software, 2009 IEEE International
714 Geoscience and Remote Sensing Symposium, 2009, IV-733-IV-736,

715 Instituto Geográfico Militar: Fotografía aérea 360 Rollo 19 Cámara RC10 Proyecto Carta Nacional N-III_1977 Escala
716 1:60000   B/N.   [online].   Accessed: 20   March   2020.   Available   from:
717 http://www.geoportaligm.gob.ec/geonetwork/srv/spa/catalog.search#/metadata/e56534b0-3b16-423e-a076-e0e41df07a81,
718 1977.

719 Instituto Geográfico Militar: Generation of geospatial information at a scale 1: 5 000 for the determination of the physical
720 fitness of the territory and urban development through the use of geotechnologies [Spanish], 2019.

721 Jalayer, F., De Risi, R., De Paola, F., Giugni, M., Manfredi, G., Gasparini, P., Topa, M. E., Yonas, N., Yeshitela, K.,
722 Nebebe, A., Cavan, G., Lindley, S., Printz, A., and Renner, F.: Probabilistic GIS-based method for delineation of urban
723 flooding risk hotspots, Natural Hazards, 73, 975-1001, 10.1007/s11069-014-1119-2, 2014.

724 James, P., Banay, R. F., Hart, J. E., and Laden, F.: A Review of the Health Benefits of Greenness, Current Epidemiology
725 Reports, 2, 131-142, 10.1007/s40471-015-0043-7, 2015.

726 Jeong, D., Kim, M., Song, K., and Lee, J.: Planning a Green Infrastructure Network to Integrate Potential Evacuation Routes
727 and the Urban Green Space in a Coastal City: The Case Study of Haeundae District, Busan, South Korea, Science of The
728 Total Environment, 761, 143179, https://doi.org/10.1016/j.scitotenv.2020.143179, 2021.

729 Kelleher, C., and McPhillips, L.: Exploring the application of topographic indices in urban areas as indicators of pluvial
730 flooding locations, Hydrological Processes, 34, 780-794, 2020.

731 Kennedy, R. E., Yang, Z., Gorelick, N., Braaten, J., Cavalcante, L., Cohen, W. B., and Healey, S.: Implementation of the
732 LandTrendr Algorithm on Google Earth Engine, Remote Sensing, 10, 691, 2018.

733 Khazai, B., Anhorn, J., Girard, T., Brink, S., Daniell, J., Bessel, T., Mühr, B., Flörchinger, V., and Kunz-Plapp, T.: Shelter
734 response and vulnerability of displaced populations in the April 25, 2015 Nepal Earthquake, Center for Disaster
735 Management and Risk Reduction Technology of the Karlsruhe Institute of Technology, and the South Asia Institute,
736 Heidelberg University, 5, 2015, 2015.

737 Kılcı, F., Kara, B. Y., and Bozkaya, B.: Locating temporary shelter areas after an earthquake: A case for Turkey, European
738 Journal of Operational Research, 243, 323-332, https://doi.org/10.1016/j.ejor.2014.11.035, 2015.

739 Kirschbaum, D., Stanley, T., and Yatheendradas, S.: Modeling landslide susceptibility over large regions with fuzzy overlay,
740 Landslides, 13, 485-496, 10.1007/s10346-015-0577-2, 2016.

741 Kumar, P., Debele, S. E., Sahani, J., Rawat, N., Marti-Cardona, B., Alfieri, S. M., Basu, B., Basu, A. S., Bowyer, P.,
742 Charizopoulos, N., Jaakko, J., Loupis, M., Menenti, M., Mickovski, S. B., Pfeiffer, J., Pilla, F., Pröll, J., Pulvirenti, B.,
743 Rutzinger, M., Sannigrahi, S., Spyrou, C., Tuomenvirta, H., Vojinovic, Z., and Zieher, T.: An overview of monitoring
744 methods for assessing the performance of nature-based solutions against natural hazards, Earth-Science Reviews, 217,
745 103603, https://doi.org/10.1016/j.earscirev.2021.103603, 2021.

746 Labib, S. M., and Harris, A.: The potentials of Sentinel-2 and LandSat-8 data in green infrastructure extraction, using object
747 based image analysis (OBIA) method, European Journal of Remote Sensing, 51, 231-240, 10.1080/22797254.2017.1419441,
748 2018.

749 Lidberg, W., Nilsson, M., Lundmark, T., and Ågren, A. M.: Evaluating preprocessing methods of digital elevation models
750 for hydrological modelling, Hydrological Processes, 31, 4660-4668, 2017.

751 Liu, Q., Ruan, X., and Shi, P.: Selection of emergency shelter sites for seismic disasters in mountainous regions: Lessons
752 from the 2008 Wenchuan Ms 8.0 Earthquake, China, Journal of Asian Earth Sciences, 40, 926-934, 2011.

753 Loughlin, S. C., Sparks, R. S. J., Sparks, S., Brown, S. K., Jenkins, S. F., and Vye-Brown, C.: Global volcanic hazards and
754 risk, Cambridge University Press, 2015.

755 Manfreda, S., Di Leo, M., and Sole, A.: Detection of flood-prone areas using digital elevation models, Journal of Hydrologic
756 Engineering, 16, 781-790, 2011.

757 Maragno, D., Gaglio, M., Robbi, M., Appiotti, F., Fano, E. A., and Gissi, E.: Fine-scale analysis of urban flooding reduction
758 from green infrastructure: An ecosystem services approach for the management of water flows, Ecological Modelling, 386,
759 1-10, https://doi.org/10.1016/j.ecolmodel.2018.08.002, 2018.

760 Markus, T., Neumann, T., Martino, A., Abdalati, W., Brunt, K., Csatho, B., Farrell, S., Fricker, H., Gardner, A., Harding, D.,
761 Jasinski, M., Kwok, R., Magruder, L., Lubin, D., Luthcke, S., Morison, J., Nelson, R., Neuenschwander, A., Palm, S.,
762 Popescu, S., Shum, C. K., Schutz, B. E., Smith, B., Yang, Y., and Zwally, J.: The Ice, Cloud, and land Elevation Satellite-2
763 (ICESat-2): Science requirements, concept, and implementation, Remote Sensing of Environment, 190, 260-273,
764 https://doi.org/10.1016/j.rse.2016.12.029, 2017.

765 Marmot, M., Friel, S., Bell, R., Houweling, T. A. J., and Taylor, S.: Closing the gap in a generation: health equity through
766 action on the social determinants of health, The Lancet, 372, 1661-1669, https://doi.org/10.1016/S0140-6736(08)61690-6,
767 2008.

768 Marselle, M. R., Bowler, D. E., Watzema, J., Eichenberg, D., Kirsten, T., and Bonn, A.: Urban street tree biodiversity and
769 antidepressant prescriptions, Scientific Reports, 10, 22445, 10.1038/s41598-020-79924-5, 2020.

770 Mattivi, P., Franci, F., Lambertini, A., and Bitelli, G.: TWI computation: a comparison of different open source GISs, Open
771 Geospatial Data, Software and Standards, 4, 1-12, 2019.

772 McDonald, R. I., Mansur, A. V., Ascensão, F., Colbert, M. l., Crossman, K., Elmqvist, T., Gonzalez, A., Güneralp, B.,
773 Haase, D., Hamann, M., Hillel, O., Huang, K., Kahnt, B., Maddox, D., Pacheco, A., Pereira, H. M., Seto, K. C., Simkin, R.,
774 Walsh, B., Werner, A. S., and Ziter, C.: Research gaps in knowledge of the impact of urban growth on biodiversity, Nature
775 Sustainability, 3, 16-24, 10.1038/s41893-019-0436-6, 2020.

776 McVittie, A., Cole, L., Wreford, A., Sgobbi, A., and Yordi, B.: Ecosystem-based solutions for disaster risk reduction:
777 Lessons from European applications of ecosystem-based adaptation measures, International Journal of Disaster Risk
778 Reduction, 32, 42-54, https://doi.org/10.1016/j.ijdrr.2017.12.014, 2018.

779 Metro Ecuador: En caso de un sismo en Quito, estos son los sitios seguros en la ciudad. Metro Ecuador. [Online]. 12
780 December. [Accessed 01 November 2021]. Available from: https://www.metroecuador.com.ec/ec/noticias/2019/05/28/caso-
781 temblor-estos-los-sitios-seguros-quito.html. 2019.

782 Millard, K., and Richardson, M.: On the Importance of Training Data Sample Selection in Random Forest Image
783 Classification: A Case Study in Peatland Ecosystem Mapping, Remote. Sens., 7, 8489-8515, 2015.

784 Ministry of Territory. Habitat and Housing.: Accidentes.
785 https://territorio.maps.arcgis.com/home/item.html?id=5270bc85cf3249b29937d25d0b363396, 2020.

786 Myint, S. W., Gober, P., Brazel, A., Grossman-Clarke, S., and Weng, Q.: Per-pixel vs. object-based classification of urban
787 land cover extraction using high spatial resolution imagery, Remote Sensing of Environment, 115, 1145-1161,
788 http://dx.doi.org/10.1016/j.rse.2010.12.017, 2011.

789 Neumann, T. A., Martino, A. J., Markus, T., Bae, S., Bock, M. R., Brenner, A. C., Brunt, K. M., Cavanaugh, J., Fernandes,
790 S. T., Hancock, D. W., Harbeck, K., Lee, J., Kurtz, N. T., Luers, P. J., Luthcke, S. B., Magruder, L., Pennington, T. A.,
791 Ramos-Izquierdo, L., Rebold, T., Skoog, J., and Thomas, T. C.: The Ice, Cloud, and Land Elevation Satellite – 2 mission: A
792 global geolocated photon product derived from the Advanced Topographic Laser Altimeter System, Remote Sensing of
793 Environment, 233, 111325, https://doi.org/10.1016/j.rse.2019.111325, 2019.

794 Neumann, T. A., A. Brenner, D. Hancock, J. Robbins, J. Saba, K. Harbeck, A. Gibbons, J. Lee, S. B. Luthcke, T. Rebold, .
795 ATLAS/ICESat-2 L2A Global Geolocated Photon Data, Version 3. Boulder, Colorado USA. NASA National Snow and Ice
796 Data Center Distributed Active Archive Center. doi: https://doi.org/10.5067/ATLAS/ATL03.003. [Accessed 7th December
797 2020]. 2020.

798 Nuth, C., and Kääb, A.: Co-registration and bias corrections of satellite elevation data sets for quantifying glacier thickness
799 change, The Cryosphere, 5, 271-290, https://doi.org/10.1016/10.5194/tc-5-271-2011, 2011.

800 Oliver-Smith, A., Alcántara-Ayala, I., I, B., and Lavell, A.: Forensic Investigations of Disasters (FORIN): a conceptual
801 framework and guide to research. Available online: http://www.irdrinternational.org/wp-content/uploads/2016/01/FORIN-2-
802 29022016.pdf
803 (accessed on 11 November 2019). 2016.

804 Olofsson, P., Foody, G. M., Stehman, S. V., and Woodcock, C. E.: Making better use of accuracy data in land change
805 studies: Estimating accuracy and area and quantifying uncertainty using stratified estimation, Remote Sensing of
806 Environment, 129, 122-131, https://doi.org/10.1016/j.rse.2012.10.031, 2013.

807 Olofsson, P., Foody, G. M., Herold, M., Stehman, S. V., Woodcock, C. E., and Wulder, M. A.: Good practices for estimating
808 area and assessing accuracy of land change, Remote Sensing of Environment, 148, 42-57,
809 https://doi.org/10.1016/j.rse.2014.02.015, 2014.

810 Onuma, A., and Tsuge, T.: Comparing green infrastructure as ecosystem-based disaster risk reduction with gray
811 infrastructure in terms of costs and benefits under uncertainty: A theoretical approach, International Journal of Disaster Risk
812 Reduction, 32, 22-28, https://doi.org/10.1016/j.ijdrr.2018.01.025, 2018.

813 Pagani, M., Garcia-Pelaez, J., Gee, R., Johnson, K., Poggi, V., Styron, R., Weatherill, G., Simionato, M., Viganò, D.,
814 Danciu, L., and Monelli, D.: Global Earthquake Model (GEM) Seismic Hazard Map (version 2018.1 - December 2018).
815 Availalbe online: https://www.globalquakemodel.org/gem-maps/global-earthquake-hazard-map (accessed 5 May 2021).
816 DOI: 10.13117/GEM-GLOBAL-SEISMIC-HAZARD-MAP-2018.1, 2018.

817 Passalacqua, P., Belmont, P., Staley, D. M., Simley, J. D., Arrowsmith, J. R., Bode, C. A., Crosby, C., DeLong, S. B., Glenn,
818 N. F., Kelly, S. A., Lague, D., Sangireddy, H., Schaffrath, K., Tarboton, D. G., Wasklewicz, T., and Wheaton, J. M.:
819 Analyzing high resolution topography for advancing the understanding of mass and energy transfer through landscapes: A
820 review, Earth-Science Reviews, 148, 174-193, http://dx.doi.org/10.1016/j.earscirev.2015.05.012, 2015.

821 Pelling, M., Maskrey, A., Ruiz, P., Hall, P., Peduzzi, P., Dao, Q.-H., Mouton, F., Herold, C., and Kluser, S.: Reducing
822 disaster risk: a challenge for development, 2004.

823 Peralta Arias, J. J., and Higueras García, E.: Evaluación sostenible de los Planes Directores de Quito. Periodo 1942-2012,
824 2016.

825 Pettorelli, N., Vik, J. O., Mysterud, A., Gaillard, J.-M., Tucker, C. J., and Stenseth, N. C.: Using the satellite-derived NDVI
826 to assess ecological responses to environmental change, Trends in Ecology & Evolution, 20, 503-510,
827 https://doi.org/10.1016/j.tree.2005.05.011, 2005.

828 Phillips, C., and Marden, M.: Reforestation Schemes to Manage Regional Landslide Risk, in: Landslide Hazard and Risk,
829 517-547, 2005.

830 Rebotier, J.: El riesgo y su gestión en Ecuador: una mirada de geografía social y política, Centro de Publicaciones Pontificia
831 Universidad Católica del Ecuador, 2016.

832 Robin, C., Samaniego, P., Le Pennec, J.-L., Mothes, P., and van der Plicht, J.: Late Holocene phases of dome growth and
833 Plinian activity at Guagua Pichincha volcano (Ecuador), Journal of Volcanology and Geothermal Research, 176, 7-15,
834 https://doi.org/10.1016/j.jvolgeores.2007.10.008, 2008.

835 Rodriguez-Galiano, V. F., Ghimire, B., Rogan, J., Chica-Olmo, M., and Rigol-Sanchez, J. P.: An assessment of the
836 effectiveness of a random forest classifier for land-cover classification, ISPRS Journal of Photogrammetry and Remote
837 Sensing, 67, 93-104, https://doi.org/10.1016/j.isprsjprs.2011.11.002, 2012.

838 Salazar, E., Henríquez, C., Sliuzas, R., and Qüense, J.: Evaluating Spatial Scenarios for Sustainable Development in Quito,
839 Ecuador, ISPRS Int. J. Geo Inf., 9, 141, 2020.

840 Salazar, E., Henríquez, C., Durán, G., Qüense, J., and Puente-Sotomayor, F.: How to Define a New Metropolitan Area? The
841 Case of Quito, Ecuador, and Contributions for Urban Planning, Land, 10, 413, 2021.

842 Salmon, N., Yépez, G., Duque, M., Yépez, M., Báez, A., Masache-Heredia, M., Mejía, G., Mejía, P., Garofalo, G., and
843 Montoya, D.: Co-design of a Nature-Based Solutions Ecosystem for Reactivating a Peri-Urban District in Quito, Ecuador, in:
844 Governance of Climate Responsive Cities: Exploring Cross-Scale Dynamics, edited by: Peker, E., and Ataöv, A., Springer
845 International Publishing, Cham, 79-104, 2021.

846 Sandholz, S., Lange, W., and Nehren, U.: Governing green change: Ecosystem-based measures for reducing landslide risk in
847 Rio de Janeiro, International Journal of Disaster Risk Reduction, 32, 75-86, https://doi.org/10.1016/j.ijdrr.2018.01.020, 2018.

848 Schneider, A., and Woodcock, C. E.: Compact, Dispersed, Fragmented, Extensive? A Comparison of Urban Growth in
849 Twenty-five Global Cities using Remotely Sensed Data, Pattern Metrics and Census Information, Urban Studies, 45, 659-
850 692, 10.1177/0042098007087340, 2008.

851 Shimpo, N., Wesener, A., and McWilliam, W.: How community gardens may contribute to community resilience following
852 an earthquake, Urban Forestry & Urban Greening, 38, 124-132, https://doi.org/10.1016/j.ufug.2018.12.002, 2019.

853 Shrestha, S. R., Sliuzas, R., and Kuffer, M.: Open spaces and risk perception in post-earthquake Kathmandu city, Applied
854 Geography, 93, 81-91, https://doi.org/10.1016/j.apgeog.2018.02.016, 2018.

855 Sierra, A.: La política de mitigación de los riesgos en las laderas de Quito: ¿qué vulnerabilidad combatir?, 2009,

856 SNI: Archivos de Informacion Geografica. Peligro Volcánico [Accessed 24 August 2020], 2020.

857 Sphere Association: The Sphere Handbook: Humanitarian Charter and Minimum Standards in Humanitarian Response,
858 fourth edition, Geneva, Switzerland,
859 www.spherestandards.org/handbook, 2018.

860 Stanley, T., and Kirschbaum, D. B.: A heuristic approach to global landslide susceptibility mapping, Natural Hazards, 87,
861 145-164, https://doi.org/10.1007/s11069-017-2757-y, 2017.

862 Styron, R.: GEMScienceTools/gem-global-active-faults: First release of 2019 (Version 2019.0), ZENODO,
863 http://doi.org/10.5281/zenodo.3376300, 2019.

864 Sudmeier-Rieux, K., Arce-Mojica, T., Boehmer, H. J., Doswald, N., Emerton, L., Friess, D. A., Galvin, S., Hagenlocher, M.,
865 James, H., Laban, P., Lacambra, C., Lange, W., McAdoo, B. G., Moos, C., Mysiak, J., Narvaez, L., Nehren, U., Peduzzi, P.,
866 Renaud, F. G., Sandholz, S., Schreyers, L., Sebesvari, Z., Tom, T., Triyanti, A., van Eijk, P., van Staveren, M., Vicarelli, M.,
867 and Walz, Y.: Scientific evidence for ecosystem-based disaster risk reduction, Nature Sustainability, 4, 803-810,
868 10.1038/s41893-021-00732-4, 2021.

869 Taylor, L., and Hochuli, D. F.: Defining greenspace: Multiple uses across multiple disciplines, Landscape and Urban
870 Planning, 158, 25-38, https://doi.org/10.1016/j.landurbplan.2016.09.024, 2017.

871 Testori, G.: Gobierno Barrial de Atucucho. An urban alternative based on self-governance and direct democracy, 2016.

872 Tidball, K. G., and Krasny, M. E.: Greening in the red zone: Disaster, Resilience and Community Greening, Springer, 2012.

873 Tucker, C. J., Holben, B. N., Elgin, J. H., and McMurtrey, J. E.: Remote sensing of total dry-matter accumulation in winter
874 wheat, Remote Sensing of Environment, 11, 171-189, https://doi.org/10.1016/0034-4257(81)90018-3, 1981.

875 UN-Habitat: The Challenge of Slums: Global Report on Human Settlements 2003. Availalbe online:
876 https://www.alnap.org/help-library/the-challenge-of-slums-global-report-on-human-settlements-2003 (accessed on 4 May
877 2021), 2003.

878 UN DESA: World Urbanization Prospects: The 2018 Revision (ST/ESA/SER.A/420). New York: United Nations., 2019.

879 UN General Assembly: Transforming our world: the 2030 Agenda for Sustainable Development. Report No. A/RES/70/1,,
880 2015.

881 Sendai   framework   for   disaster   risk   reduction   2015   -   2030.:
882 https://www.preventionweb.net/files/43291_sendaiframeworkfordrren.pdf, access: 05 February 2020, 2015.

883 UNDRR: Ecosystem-Based Disaster Risk Reduction: Implementing Nature-based Solutions for Resilience, United Nations
884 Office for Disaster Risk Reduction – Regional Office for Asia and the Pacific, Bangkok, Thailand, 2020.

885 Valcárcel, J., Despotaki, V., Burton, C., Yepes-Estrada, C., Silva, V., and Villacis, C.: Integrated Assessment of Earthquake
886 Risk in Quito, Ecuador Using Openquake, 16th World Conference on Earthquake Engineering, 16WCEE 2017, 2017,

887 Valencia, V. H., Levin, G., and Hansen, H. S.: Modelling the spatial extent of urban growth using a cellular automata-based
888 model: a case study for Quito, Ecuador, Geografisk Tidsskrift-Danish Journal of Geography, 120, 156-173,
889 10.1080/00167223.2020.1823867, 2020.

890 Vidal, X., Burgos, L., and Zevallos, O.: 11 Protection and environmental restoration of the slopes of Pichincha in Quito,
891 Ecuador, Water and Cities in Latin America: Challenges for Sustainable Development, 181, 2015.

892 Vincenti, S. S., Zuleta, D., Moscoso, V., Jácome, P., Palacios, E., and Villacís, M.: Análisis estadístico de datos
893 meteorológicos mensuales y diarios para la determinación de variabilidad climática y cambio climático en el Distrito
894 Metropolitano de Quito, La Granja, 16, 23-47, 2012.

895 WHO Regional Office for Europe: Urban green spaces and health., 2016.

896 Wilson, T. M., Stewart, C., Sword-Daniels, V., Leonard, G. S., Johnston, D. M., Cole, J. W., Wardman, J., Wilson, G., and
897 Barnard, S. T.: Volcanic ash impacts on critical infrastructure, Physics and Chemistry of the Earth, Parts A/B/C, 45-46, 5-23,
898 https://doi.org/10.1016/j.pce.2011.06.006, 2012.

899 Wolch, J. R., Byrne, J., and Newell, J. P.: Urban green space, public health, and environmental justice: The challenge of
900 making cities 'just green enough', Landscape and Urban Planning, 125, 234-244,
901 https://doi.org/10.1016/j.landurbplan.2014.01.017, 2014.

902 Zalakeviciute, R., López-Villada, J., and Rybarczyk, Y.: Contrasted Effects of Relative Humidity and Precipitation on Urban
903 PM2.5 Pollution in High Elevation Urban Areas, Sustainability, 10, 2064, 2018.

904 Zambrano-Barragán, C., Zevallos, O., Villacís, M., and Enríquez, D.: Quito's Climate Change Strategy: A Response to
905 Climate Change in the Metropolitan District of Quito, Ecuador, in: Resilient Cities, Dordrecht, 2011, 515-529,

906 Zhu, Z., Gallant, A. L., Woodcock, C. E., Pengra, B., Olofsson, P., Loveland, T. R., Jin, S., Dahal, D., Yang, L., and Auch,
907 R. F.: Optimizing selection of training and auxiliary data for operational land cover classification for the LCMAP initiative,
908 ISPRS Journal of Photogrammetry and Remote Sensing, 122, 206-221, https://doi.org/10.1016/j.isprsjprs.2016.11.004, 2016.
909